Journal of Engineering Research and Reports

Volume 24, Issue 7, Page 18-42, 2023; Article no.JERR.97150
ISSN: 2582-2926

Observer-based Finite-time Event-triggered Asynchronous Sliding Mode Control for Interval Type-II Fuzzy Semi-Markov Jump Systems with Quantization and Fading Channels

Jinhua Jiang [a], **Mengzhuo Luo** [a*] **and Sisi Lin** [b]

[a] *College of Science, Guilin University of Technology, Guilin, Guangxi, 541004, P. R. China.*
[b] *School of Mathematics and Statistics, Shaoguan University, Shaoguan, 512005, P. R. China.*

Authors' contributions

This work was carried out in collaboration among all authors. All authors read and approved the final manuscript.

Article Information

DOI: 10.9734/JERR/2023/v24i7829

Open Peer Review History:
This journal follows the Advanced Open Peer Review policy. Identity of the Reviewers, Editor(s) and additional Reviewers, peer review comments, different versions of the manuscript, comments of the editors, etc are available here: https://www.sdiarticle5.com/review-history/97150

Original Research Article

Received: 06/01/2023
Accepted: 03/03/2023
Published: 09/03/2023

ABSTRACT

In this paper, we investigate the finite-time event-triggered sliding mode control(SMC) issue of a class of interval type-II fuzzy semi-Markov jump systems affected by quantization and fading channels. Firstly, the data needs to be quantized by logarithmic quantizers before being transmitted over the channel. To alleviate network pressure, a periodic event-triggered scheme is introduced to govern whether the data are sent to the sensor-to-controller(S/C) channel or not. As the transmitted data passes through the S/C channel, it could undergo fading. Then, considering the asynchronous issue between the system mode and the controller mode, an

**Corresponding author: Email: zhuozhuohuahua@163.com;*

asynchronous control scheme is applied; Thereafter, a feasible fuzzy observer-based SMC law is developed, which enables the state trajectories of the system to reach the specified sliding surface within finite-time; And with the aid of the time partition strategy, sufficient conditions for the system to be bounded in finite-time during the arrival and sliding stages are derived. Besides, by means of the linear matrix inequality(LMI) toolbox, the controller and the observer gains are computed. Finally, the advantages of the SMC strategy are validated by emulation products.

Keywords: Finite-time sliding mode control; periodic event-triggered scheme(PETS); quantization; fading channel (FC); interval type-II fuzzy semi-Markov jump systems.

1 INTRODUCTION

In actuality, a lot of control systems have nonlinear characteristics, which makes modeling them challenging. The Takagi-Sugeno (T-S) fuzzy model, fortunately, is an fabulous platform for approximating nonlinear systems since it combines local linear subsystems and membership functions [1]-[2]. It is undeniable that the traditional T-S fuzzy model, also known to type-I [3]-[4], is incapable of eliminating uncertainty using a simple modeling technique. Fortunately, such prospective strategy(by other words, type-II/IT2 fuzzy system mentioned throughout [5]-[6] compensates for the shortcoming. In particular, thanks to type-II fuzzy model, it's upper with lower membership functions(MFs) bounds may efficiently extract the parameter uncertainty.

Markov jump systems(MJSs) are widely used throughout the engineering field, from electrical applications to ecosystems to wireless networks [7]-[9], due to their potent willingness to represent systems with sudden changes in structure or parameters. The switching of the interconnected subsystems that make up MJSs is controlled by the Markov process [10]-[11]. In Markovian jump systems, the transition rate of Markovian process is constant, which has a definite limitation as a result of each subsystem's sojourn time following an exponential distribution. To remedy the deficiency, a semi-Markov process with time-varying transition rates is proposed to simulate stochastic switching. In light of this, in comparison to MJSs [12]-[13], semi-Markov jump systems (S-MJSs) have a wider range of potential applications. As a result, the control issues with S-MJSs have sparked continued research interest, and significant accomplishments have been published in a variety of fields [14]-[16].

The system mode should have been synchronized with the controller mode at all times [17] because it is typically anticipated that the information about the system mode may be retrieved instantly by the controller in the aforemen-tioned S-MJSs. However, it is challenging to put this premise into practice in the majority of real-world scenarios. Out-of-sync behavior between the system mode and the controller mode [18] may be brought on by certain abnormal circumstances like data missing, delayed transfer and random jamming. Generic control approach is therefore no longer appropriate in this situation. Preset conditional probability for controlling changes between the system mode and the controller mode is imported in response to this phenomenon, and the asynchronous control method has since drawn more attention [19]. Additionally, a non-synchronous approach has been broadly applied in filtering field [20]. However, with regard to the asynchronous SMC issue of S-MJSs, it remains open, prompting us to bridge the gap. This is the main motivation for writing this paper.

As technology evolves, additional data is transferred between the various parts of the system through bandwidth-limited common communication networks. A key issue is finding ways to decrease resource depletion and reduce the load on transportation. One plausible approach is to use an event-triggered scheme to ascertain if the signal is to be transmitted[21]-[23]. In addition, some significant foundations for event-triggered SMC were achieved in [24]-[25] and expanded upon multiagent systems in [26]-[28]. The avoidance of Zeno phenomenon in sequential time systems remains an invaluable problem in a community of event-triggered controls. In addition, an obvious obstacle to combining interval type-II fuzzy systems with a periodic event-triggered scheme is that the membership functions present in the primitive fuzzy model as well as the premise variables cannot be directly obtained directly to design the controller. In particular, the problem of dealing with event-triggered SMC for continuous-time interval type-II fuzzy S-MJSs in an immeasurable state

is quite competitive, which is a significant impetus for conducting such task.

Besides, by making data quantifiable, bandwidth can be better allocated and the stress resulting from data overload can be alleviated, as stated in [29]. Therefore, we also consider quantification data simultaneously. Nevertheless, quantification errors have a significant impact on the capacity of the system and at times destabilization [30], which merits further discussion. As a result, it is of great significance to find the correct method to solve the quantification errors.

The signal fading phenomenon [31]-[32] in the communication network is another problem. It is caused by a number of unavoidable physical variables, such as shadowing and multipath. There have been several studies about FC for discrete-time systems [33] and continuous-time systems [34]. Nevertheless, the application of event-triggered protocols to interval type-II fuzzy semi-Markovian jump systems affected by FC, quantization and immeasurable states, there are not many relevant research results. This is another research motivation of this paper.

What's more, sliding mode control (SMC), alternatively known as variational configuration control, is in essence a subset of nonlinear control. Throughout the kinetic procedure, the relationship with the current state of the system could be purposefully changed so that the system is deleted according to the predefined state trajectory of the sliding mode. Given that sliding mode can be structured, is unaffected by target parametric and interference, and provides merits such as quick feedback and impervious to parametric changes and interference, it has been widely used in power systems, automated fabrication technology, automotive generators, with additional domains [35]-[37]. In [38]-[40] , it is highlighted that Lyapunov stability takes into account the fact that the system's trajectory achieves a balance point within an infinitesimal time lapse. These articles only focus on the infinite-time reachability, but in engineering applications, there is an urgent need to actuate the trajectory of the system onto a specified sliding surface within a limited timespan. Consequently, a growing interest in the field of finite-time stability (FTS) and finite-time boundedness (FTB) conceptions has been observed in the recent couple of years, following the increase in efficiency of practical systems. In [41], FTB and reachability of MJSs with timelags are discussed. Besides, scholars have also extended the finite-time theory to fuzzy systems [42], multi-agent system systems [43], randomly switched systems[44] and so on.

In consideration of the above discussion, the issue of observer-based finite-time event-triggered asynchronous sliding mode control for interval type-II fuzzy S-MJSs with quantization and fading channels, which has greatly aroused our attention. The key contributions to this article are outlined below:

1. The PETS discussed in this article is designed on the basis of quantization of the data, which makes it more practically meaningful compared to those results that do not quantify the primitive data.
2. Through the fading signals available under the PETS, a state observer-based PET SMC scheme is designed in this paper, in which the membership functions(MFs) are only dependent on the estimation of the state rather than the primitive system state.
3. Given the influence of quantization, PETS and FC, the concept of FTB is introduced to deal with the mismatched MFs, the asynchronous phenomenon, the exterior interferences, actuator failures, and channel fading phenomenon. By exploiting the developed control strategy, the trajectories of the interval type-II fuzzy S-MJSs are not only guaranteed to reach the specified sliding surface in finite-time, but also sufficient conditions for the system to be bounded in finite-time are derived. At the same time, the Zeno phenomenon is eliminated because the PETS guarantees the minimum trigger interval.

Notations: The symbols applicable in the present paper are generic. $\lambda_{\max}(B)$ means the maximum eigenvalue of matrix B, with $\|B\|$ represents the Euclidean norm of B. $E\{\cdot\}$ indicates the mathematical expectation. $B > 0$ represents that B is symmetric positive-definite. "$*$" represents the symmetric block for a symmetric matrix. $sgn(b)$ represents the sign function that equals 1 when $b > 0$, equals 0 when b = 0.

2 PROBLEM FORMULATION AND PRELIMINARIES

2.1 System Description

With respect to the probabilistic space $(\text{Ç}, \text{Ł}, \Pr)$, the nonlinear S-MJSs with external disturbance are considered via the T-S fuzzy model presented below:
Set rules i: IF $\urcorner_1(x(t))$ is $\aleph_1^i$,..., and $\urcorner_\varrho(x(t))$ is $\aleph_\varrho^i$, THEN

$$\begin{cases} \dot{x}(t) = A_i(r(t))x(t) + B_i(r(t))\left(f(x(t), r(t), t) + u(t)\right) + D_i(r(t))w(t) \\ y(t) = C(r(t))x(t) \end{cases} \tag{1}$$

where $\urcorner_\jmath(x(t))$ is the premise variable, $\aleph_\jmath^i$ represents the fuzzy aggregations, $i \in \digamma = \{1, 2, \ldots, v\}, \jmath \in \Bbbm = \{1, 2, \ldots, \varrho\}$ and ϱ and v are the number of premise variables and fuzzy rules, separately. $u(t)$ and $x(t)$ signify the control input and the system state, separately; $y(t)$ is the output vector; $w(t)$ is the exterior interference pertaing to $L_2[0, \infty)$; $f(x(t), r(t), t)$ is the faults signals for non-linear actuators. The firing intensity is for the rule i specified as the below given set of intervals: $\eta_i(x(t)) = \left[\underline{\eta}_i(x(t)), \overline{\eta}_i(x(t))\right]$ with

$$\underline{\eta}_i(x(t)) = \prod_{\jmath=1}^{\varrho} \underline{\mu}_{\aleph_\jmath^i}\left(\urcorner_\jmath(x(t))\right) > 0, \overline{\eta}_i(x(t)) = \prod_{\jmath=1}^{\varrho} \overline{\mu}_{\aleph_\jmath^i}\left(\urcorner_\jmath(x(t))\right) > 0,$$

where $\underline{\mu}_{\aleph_\jmath^i}\left(\urcorner_\jmath(x(t))\right)$ and $\overline{\mu}_{\aleph_\jmath^i}\left(\urcorner_\jmath(x(t))\right) \in [0, 1)$ are the lower and upper grade of the MFs, satisfying $\underline{\mu}_{\aleph_\jmath^i}\left(\urcorner_\jmath(x(t))\right) \leq \overline{\mu}_{\aleph_\jmath^i}\left(\urcorner_\jmath(x(t))\right)$. $\{r(t), \hbar\}_{t\geq 0} \triangleq \{r_s, \hbar_s\}_{s\in N_1}$ is a semi-Markovian process with its values within a finite set $N_1 \triangleq \{1, 2, \ldots, M_1\}$. Then, the transition rate matrix $||_1(\hbar) \triangleq [\pi_{mn}(\hbar)]_{M_1\times M_1}$ is determined by

$$\begin{cases} \Pr\{r_{s+1} = n, \hbar_{s+1} \leq \hbar + \Delta | \, r_s = m, \hbar_{s+1} > \hbar\} \\ = \pi_{mn}(\hbar)\Delta + o(\Delta), m \neq n \\ \Pr\{r_{s+1} = n, \hbar_{s+1} > h + \Delta | \, r_s = m, \hbar_{s+1} > \hbar\} \\ = 1 + \pi_{mn}(\hbar)\Delta + o(\Delta), m = n \end{cases}$$

where $\lim_{\Delta\to 0}(o(\Delta)/\Delta) = 0$; $\pi_{mn}(\hbar) \geq 0$, with regard to $m \neq n$, represents the transition rate from mode m at time t to mode n at time $t + \Delta$ and $\pi_{mn}(\hbar) = -\sum_{n\in N_1, m\neq n} \pi_{mn}(\hbar)$.

To the whole $r(t) \triangleq m$, we define $A_{im} \triangleq A_i(r(t)), B_{im} \triangleq B_i(r(t)), C_m \triangleq C(r(t)), D_{im} \triangleq D_i(r(t))$, $f_m(x(t), t) \triangleq f(x(t), r(t), t)$ to simplier the notations. Thus, the overall considered fuzzy S-MJSs can be formulated via the below T-S fuzzy model:

$$\begin{cases} \dot{x}(t) = \sum_{i=1}^{v} \eta_i(x(t))\left[A_{im}x(t) + B_{im}\left(f_m(x(t), t) + u(t)\right) + D_{im}w(t)\right] \\ y(t) = C_m x(t) \end{cases} \tag{2}$$

with

$$\eta_i(x(t)) = \underline{\eta}_i(x(t))\underline{\vartheta}_i(x(t)) + \overline{\eta}_i(x(t))\overline{\vartheta}_i(x(t))$$
$$\underline{\vartheta}_i(x(t)), \overline{\vartheta}_i(x(t)) \in [0, 1], \underline{\vartheta}_i(x(t)) + \overline{\vartheta}_i(x(t)) = 1, \sum_{i=1}^{v} \eta_i(x(t)) = 1$$

Where the the nonlinearity functions $\underline{\vartheta}_i(x(t))$ and $\overline{\vartheta}_i(x(t))$ enable uncertainty in parameters to be trapped, A_{im}, B_{im}, C_m, D_{im} are known matrices with proper dimensionalities.

2.2 Communication Network Based on Quantization, PETS and an Asynchronous Control Plan

To sieve through the required data, the logarithmic quantizers, PETS are introduced to save network bandwidth on the article. One key issue for channels is that the transmitted signal should be quantized firstly. Inspired by the

literature[29]-[30], to better describe the quantization error, we give the logarithmic quantizer model and utilize the sector bound method to deal with this problem. The quantization level β_c is given as:

$$\upsilon = \{\pm\beta_c : \beta_c = \psi_c\beta_0, c = \pm1, \pm2, \dots\} \bigcup \{\pm\beta_0\} \bigcup \{0\}, \beta_0 > 0, 0 < \psi < 1$$

where ψ represents the quantization density that greatly affects the quantization precision. Then, the following quantization function shows the quantized signal of $y_n(kh)$:

$$q\left(y_n(kh)\right) = \begin{cases} \beta_c, & \frac{\beta_c}{1+\varphi} < y_n(kh) < \frac{\beta_c}{1-\varphi} \\ 0, & y_n(kh) = 0, \\ -q\left(-y_n(kh)\right), & y_n(kh) < 0 \end{cases} \tag{3}$$

With h reprensents sampling period and $\varphi = 1 - \psi/1 + \psi$. By utilizing the sector bound method, the quantization error is given as follows:

$$\Delta q_n(kh) y_n(kh) = q\left(y_n(kh)\right) - y_n(kh) \tag{4}$$

Then, the quantized output signal of $y(k)$ can be further rewritten as:

$$Q(y(kh)) = (I + \Delta Q(kh)) y(kh) \tag{5}$$

with $\Delta Q(kh) = diag\left\{\Delta q_1(kh), \Delta q_2(kh), \dots, \Delta q_N(kh)\right\}$. Besides, from the structure of logarithmic quantizer, it can be easily verified that $|\Delta q_n(kh) y_n(kh)| \leq \varphi |y_n(kh)|$
Meanwhile, we can further achieve the norm-bounded condition $\|\Delta Q(kh)\| \leq \varphi$.

Remark 2.1. *Noticeably, we use static logarithmic quantizers here, which promote better bandwidth usage and lessen the burden on data. Nevertheless, with the quantification process comes quantification error, which is strongly correlated with quantification density. With other words, higher quantification density means lower quantification error. Further, this also implies an ability to withstand increased amounts of data and provide greater system capability.*

Then, we use a periodic event-triggered (PET) scheme to further relieve network pressure. Therefore, the event generator between a sampler and Zero-order-hold(ZOH) is employed to decide whether to transmit the sampled data $Q(y((k+l)h))$ to the controller through the judgment rule as follows:

$$\begin{aligned} &\left[Q(y((k+l)h)) - Q(y(kh))\right]^T \Phi_m \left[Q(y((k+l)h)) - Q(y(kh))\right] \\ &\quad \leq \alpha(m) Q^T(y((k+l)h)) \Phi_m Q(y((k+l)h)) \end{aligned} \tag{6}$$

Where $l = 1, 2, \dots, \alpha(m) \in [0, 1)$ are known triggering parameters, $\Phi_m > 0$ is the event-triggered matrix that requires determination.

Remark 2.2. *According to the judgment rule (6), assume that $t_k h (k = 0, 1, 2, \dots)$ represents the release times, where $t_0 = 0$ is the initial time. Therefore, $s_k h = t_{k+1} h - t_k h$ can represent the release period corresponding to the sampling period given by the event generator in (6). Assume that the time-varying network-induced delay is $\rho_k \in [0, \bar{\rho}]$, where $\bar{\rho}$ is a positive real parameter. Hence, the triggered data $Q(y(t_0 h)), Q(y(t_1 h)), Q(y(t_2 h)), \dots$ can reach the SMC at $t_0 h + \rho_0, t_1 h + \rho_1, t_2 h + \rho_2, \dots$ instants respectively.*

Remark 2.3. *In order to further save network bandwidth and make full use of network resources, we use the event generator to transmit system communication data under a PETS. The set of the release instants is a subset for sampled time series, that is, $\{t_0 h, t_1 h, t_2 h, \dots\} \subseteq \{0, h, 2h, \dots\}$, which means that the minimum inter-event time $\min_k \{t_{k+1} h - t_k h\}$ is lower bounded at the sampling period h. Therefore, Zeno behavior will not occur.*

Based on the analysis above and considering the effect of the network-induced transmission delay, here provides the following two conditions:

Case I: If $t_k h + h + \bar{\rho} \geq t_{k+1} h + \rho_{k+1}$, denote network-induced time-delay $\rho(t)$ as: $\rho(t) = t - t_k h$,
$t \in [t_k h + \rho_k, t_{k+1} h + \rho_{k+1})$. As a result, $\rho_k \leq \rho(t) \leq (t_{k+1} - t_k) h + \rho_{k+1} \leq h + \bar{\rho}$.

Case II: If $t_k h + h + \bar{\rho} < t_{k+1} h + \rho_{k+1}$, take two intervals:

$$[t_k h + \rho_k, t_k h + h + \bar{\rho}), [t_k h + \xi h + \bar{\rho}, t_k h + \xi h + h + \bar{\rho}).$$

Due to $\rho_k \leq \bar{\rho}$, ξ can be selected satisfying: $t_k h + \xi h + \bar{\rho} < t_{k+1} h + \rho_{k+1} \leq t_k h + \xi h + h + \bar{\rho}$.

$Q(y(t_k h))$ and $Q(y(t_k h + \zeta h))$ with $\zeta = 1, 2, \ldots, \xi$ meet that:

$$\begin{aligned} &[Q(y(t_k h + \zeta h)) - Q(y(t_k h))]^T \Phi_m [Q(y(t_k h + \zeta h)) - Q(y(t_k h))] \\ &\leq \alpha(m) Q^T(y(t_k h + \zeta h)) \Phi_m Q(y(t_k h + \zeta h)) \end{aligned} \tag{7}$$

Let

$$\begin{cases} L_{0,k} = [t_k h + \rho_k, t_k h + h + \bar{\rho}) \\ L_{\zeta,k} = [t_k h + \zeta h + \rho, t_k h + \zeta h + h + \bar{\rho})) \\ L_{\xi,k} = [t_k h + \xi h + \bar{\rho}, t_{k+1} h + \rho_{k+1}) \end{cases}$$

where $\zeta = 1, 2, \ldots, \xi - 1$. Thus

$$[t_k h + \rho_k, t_{k+1} h + \rho_{k+1}) = \bigcup_{\zeta=1}^{\zeta=\xi} L_{\zeta,k}$$

Define

$$\rho(t) = \begin{cases} t - t_k h & t \in L_{0,k} \\ t - t_k h - \zeta h & t \in L_{\zeta,k} \\ t - t_k h - \xi h & t \in L_{\xi,k} \end{cases} \tag{8}$$

As a result:

$$\begin{cases} \rho_k \leq \rho(t) \leq h + \bar{\rho}, & t \in L_{0,k} \\ \rho_k \leq \bar{\rho} \leq \rho(t) \leq h + \bar{\rho}, & t \in L_{\zeta,k} \\ \rho_k \leq \bar{\rho} \leq \rho(t) \leq h + \bar{\rho}, & t \in L_{\xi,k} \end{cases}$$

Therefore, we have

$$0 \leq \rho_k \leq \rho(t) \leq h + \bar{\rho} \triangleq \rho_M, t \in [t_k h + \rho_k, t_{k+1} h + \rho_{k+1})$$

For **case I**, denote $e_k(t) = 0$

And for **case II**, denote

$$e_k(t) = \begin{cases} 0 & t \in L_0 \\ Q(y(t_k h + \zeta h)) - Q(y(t_k h)) & t \in L_\zeta \\ Q(y(t_k h + \xi h)) - Q(y(t_k h)) & t \in L_\xi \end{cases} \tag{9}$$

where $\dot{\rho}(t) \leq g$.

Remark 2.4. *Through the above analysis, system (2) is transformed into a time-delay system due to the latency caused by network. In line with triggered schemes (7)-(9), for* $t \in [t_k h + \rho_k, t_{k+1} h + \rho_{k+1})$*, one can deduce that*

$$e_k^T(t) \Phi_m e_k(t) \leq \alpha_m Q^T(y(t - \rho(t))) \Phi_m Q(y(t - \rho(t))) \tag{10}$$

Since signals are sent only at certain trigger instants, PETS can indeed mitigate restricted communicating resources by decreasing the transfer frequency. Considering real scenario on networking transport, the signal $Q(y(t_k h))$ released through one common communication channel, it is likely to be affected by below FC:

$$\bar{y}(t_k h) = \lambda(t_k h) Q(y(t_k h)) \tag{11}$$

where $\lambda(t_k h) \in [0, 1)$ is a stochastic variable with mathematical expectation $\bar{\lambda}$, which have the ability to represent the stochastic fading behavior. For this article, only statistical information regarding the controller design is required, namely the mathematical expectation.

According to the characteristic of the ZOH, the input data $\bar{y}(t)$ for the observer can be expressed as

$$\bar{y}(t) = \bar{y}\left(t_k h\right), t \in \left[t_k h, t_{k+1} h\right) \tag{12}$$

Remark 2.5. *While some effective transfer precautions are available to lessen the load of transmission as well as finite communication resources in the network setting, a few network-induced phenomenon, just like channel fading, can be brought about. For this reason, the quantization, the PETS as well as the attenuation parameter are all considered with respect to the task. It makes the research practically more relevant and technically more challenging, where a critical point is that only the transmitted fading data $\bar{y}(t)$ can be used by the controller.*

When it comes to designing fuzzy controller for interval type-II fuzzy S-MJSs, because we use a PETS with delay, the controller may not get complete mode information about the system in a timely manner. Nevertheless, in the design of the controller, if the mode information of the system is completely discarded, it may increase the probability of system instability. Considering this situation, we introduce a non-synchronous control plan. With the introduction of a conditionally probability that depends on the mode information of the system, the controller can estimate the determined system mode information generated in the semi-Markovian evolutionary of the system. Therefore, the designed controller mode is in indirect correlation and asynchronous to the system mode. Denoting the controller mode as $\tau(t)$, the link in $\tau(t)$ and $r(t)$ is dominated by the conditional probability matrix $||_2 \triangleq \left[\hat{\pi}_{ml}\right]_{m\in N_1, l\in N_2}$,

$$\hat{\pi}_{ml} = \Pr\{\tau(t) = l \mid r(t) = m\}$$

where $l \in N_2 \triangleq \{1, 2, \ldots, M_2\}$, for $\forall m \in N_1, 0 \leq \hat{\pi}_{ml} \leq 1$ and $\sum_{l\in N_2} \hat{\pi}_{ml} = 1$.

Remark 2.6. *Generally speaking, it is considered that the mode of the system and the mode of the controller are switched synchronously, but this is difficult to achieve in practice. Since we consider a PETS with delay, there is a transmission delay between the system and the controller, which can be regarded as the asynchronous phenomenon.*

Remark 2.7. *The overall control structure framework of event-triggered asynchronous SMC for IT2 fuzzy S-MJSs is shown in Fig.1. At the same time, considering the pressure of data transmission borne by the communication network. Correspondingly, the asynchronous control scheme and the PETS are used for mitigating the impact of time lag in data transmission and finite bandwidth, separately. Next, a fuzzy SMC law with quantization, PETS and the asynchronous control plan is to be designed for the current system to realize the mean-square finite-time bounded of the closed-loop system(CLS) affected by the influence of undetectable state and FC.*

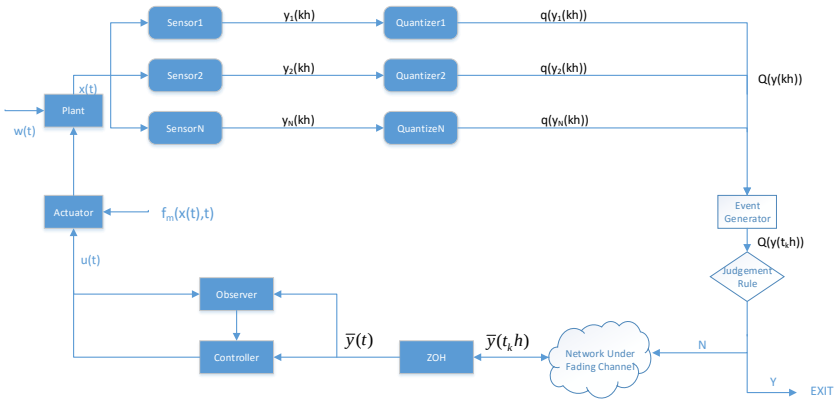

Fig.1. The overall control structure framework of event-triggered asynchronous SMC for IT2 fuzzy S-MJSs

2.3 Observer Design under Networked Communication

For the construction of an implementable state observer, there are two points that require consideration: (I) Because system state is not available, the fuzzy observer cannot be constructed directly utilizing the premise variables of IT2 fuzzy model. (II) Under quantization (5), the PETS (6) with the FC (11)-(12), it is merely possible for the observer to use the fading signal $\bar{y}(t)$. Hereafter, an ambiguous observer is in the design by using the existing fading signal $\bar{y}(t)$ and the estimation of the state-based premise variables:
If $\urcorner_1(\hat{x}(t))$ is $\aleph_1^i$,... and $\urcorner_\varrho(\hat{x}(t))$ is $\aleph_\varrho^i$,THEN

$$\begin{cases} \dot{\hat{x}}(t) = A_{im}\hat{x}(t) + B_{im}f_m(\hat{x}(t),t) + B_{im}u(t) + L_{jm}(\bar{y}(t) - \hat{y}(t-\rho(t))) \\ \hat{y}(t-\rho(t)) = C_m\hat{x}(t-\rho(t)) \end{cases} \tag{13}$$

Where $\hat{x}(t)$ represents an estimate of the $x(t)$, the gain matrix L_{jm} is to be determined afterwards. The globally ambiguous observer is deduced:

$$\begin{cases} \dot{\hat{x}}(t) = \sum\limits_{i=1}^{v}\sum\limits_{j=1}^{v}\eta_i\theta_j\left[A_{im}\hat{x}(t) + B_{im}f_m(\hat{x}(t),t) + B_{im}u(t) + L_{jm}(\bar{y}(t) - \hat{y}(t-\rho(t)))\right] \\ \hat{y}(t-\rho(t)) = C_m\hat{x}(t-\rho(t)) \end{cases} \tag{14}$$

For the sake of simplifying the notation, we define $\sum\limits_{i=1}^{v}\sum\limits_{j=1}^{v}\eta_i\theta_j \triangleq \sum\limits_{i=1}^{v}\sum\limits_{j=1}^{v}\eta_i(x(t))\theta_j(\hat{x}(t_kh))$, where $\theta_i(\hat{x}(t)) = \underline{\eta}_i(\hat{x}(t))\underline{d}_i(\hat{x}(t)) + \overline{\eta}_i(\hat{x}(t))\overline{d}_i(\hat{x}(t))$, $\underline{d}_i(\hat{x}(t))$ and $\overline{d}_i(\hat{x}(t))$ whose selection depend on the requirements for the actual application. It is worth highlighting that via using the predicted value as well as the known MFs boundaries in ambiguous system, we design the MFs of the observer as a replacement for the non-available MFs $\eta(x(t))$.

Remark 2.8. *According to the PETS (6)-(10), it is merely the signal released at the moment of triggering that is usable. In addition, the signals released are affected by attenuation phenomenon. Thus, state observer (14) is constructed by maintaining a constant fading release signal of $\bar{y}(t)$ between two triggering instant. Unlike the existing ambiguous observer which has its basis in output $y(t)$, the fading signal $\bar{y}(t)$ in state observer (14) reflects the effects of quantization, PET conditions, and fading environments, which makes control design difficult. Consequently, the sufficient conditions of stability in* ***Theorem 3.2*** *and* ***Theorem 3.3*** *are related to quantized parameters, PETS as well as FC .*

Define the estimation error $\tilde{x}(t) = x(t) - \hat{x}(t)$, by means of (2) with (14), the error system can be derived as follows:

$$\begin{aligned} \dot{\tilde{x}}(t) = &\sum_{i=1}^{v}\sum_{j=1}^{v}\eta_i\theta_j\left[A_{im}\tilde{x}(t) - L_{jm}C_m\tilde{x}(t-\rho(t)) + \lambda\left(t_kh\right)L_{jm}e_k(t)\right. \\ &\left.-\lambda\left(t_kh\right)L_{jm}Q\left(y\left(t_kh+\varepsilon h\right)\right) + L_{jm}y(t-\rho(t))\right] + \bar{w}(t) \end{aligned} \tag{15}$$

with

$$\begin{aligned} \bar{w}(t) &= \sum_{i=1}^{v}\sum_{j=1}^{v}\left[\left(\eta_i - \eta_i\theta_j\right)\left(A_{im}x(t) + B_{im}\left(f_m(\hat{x}(t),t) + u(t)\right)\right) + \eta_iD_{im}w(t)\right] \\ \varepsilon &= 0,1,\ldots,\xi. \end{aligned}$$

which could be regarded to be a resultant error term. Within the article, the resultant error term $\bar{w}(t)$ is hypothesized to fulfill $\|\bar{w}(t)\| < +\infty$. Besides, the control input $u(t)$ depends on the state of the system and has its own boundaries. Therefore, we can derive that

$$\|\bar{w}(t)\| \leq 2\max_i\left(\left(\|A_{im}\| + \sigma_m\|B_{im}\|\right)\|x(t)\| + \|B_{im}\|\|u(t)\|\right) + \max_i\|D_{im}\|\,\overline{w} < +\infty$$

Assumption 2.1. *[14] It is assumed that the fault signal of the nonlinear actuator is norm-bounded and subject to the below constraint:*

$$\|f_m(x(t),t)\| \leq \sigma_m\|x(t)\| \tag{16}$$

where $\sigma_m(m \in N_1)$ is a known positive scalar.

Assumption 2.2. *$\bar{w}(t)$ is described throughout the article as*

$$\Omega_{[0,T],\ell} = \left\{ \bar{w}(t) \in L_{2,[0,T]} : \int_0^T \bar{w}^T(s)\bar{w}(s)ds \leq \ell \right\} \tag{17}$$

with known positive scalar ℓ.

Lemma 2.1. *[41] Considering real matrices $\eth$ and $\approx$ which have suitable dimensionality, with respect to any scalar $\blacklozenge > 0$, the following inequality forms*

$$\eth^T \approx + \approx^T \eth \leq \eth^T \blacklozenge^{-1} \eth + \approx^T \blacklozenge \approx \tag{18}$$

Definition 2.1. *[41] The system is finite-time boundedness about $(c_1, c_2, [0,T], \mathbb{W}, \Omega_{[0,T],\ell})$, if exist the invariants $c_1 > 0$, $c_2 > 0$ with $c_1 < c_2$, the matrix $\mathbb{W} > 0$ with the finite-time interval $[0,T]$ enables*

$$\sup_{-\bar{\rho} \leq s < 0} E\left\{ x^T(s)\mathbb{W}x(s), \dot{x}^T(s)\mathbb{W}\dot{x}(s) \right\} \leq c_1 \Rightarrow E\left\{ x^T(t)\mathbb{W}x(t) \right\} < c_2, \forall t \in [0,T] \tag{19}$$

3 MAIN RESULTS

3.1 Sliding Surface Design

The sliding surface is given based on the estimation of the states:

$$s(t) = G_m\hat{x}(t) - G_m \int_0^t \sum_{i=1}^{v} \theta_i(\hat{x}(\xi)) \left(A_{im} + B_{im}K_{ml}\right) \hat{x}(\xi)d\xi \tag{20}$$

where the matrix $K_{ml} \in R^{m\times n}$ is designed later, $G_m \in R^{m\times n}$ is elected to guarantee G_mB_{im} is nonsingular, $i \in F$, $m \in N_1$.

Combining (14) and (20),one has:

$$\dot{s}(t) = \sum_{i=1}^{v}\sum_{j=1}^{v} \eta_i\theta_j \left[G_mB_{im}\left(f_m(\hat{x}(t),t) + u(t)\right) - G_mB_{im}K_{ml}\hat{x}(t) + G_mL_{jm}(\bar{y}(t) - \hat{y}(t-\rho(t)))\right] \tag{21}$$

Consequently, combined with (21), we deduce the following equivalent control law:

$$u_{eq}(t) = \sum_{i=1}^{v}\sum_{j=1}^{v} \eta_i\theta_j[-f_m(\hat{x}(t),t) + K_{ml}\hat{x}(t) - \left(G_mB_{im}\right)^{-1} G_mL_{jm}(\bar{y}(t) - \hat{y}(t-\rho(t)))] \tag{22}$$

By substitution of the equation (22) to (14), the sliding mode dynamics is obtained

$$\dot{\hat{x}}(t) = \sum_{i=1}^{v}\sum_{j=1}^{v} \eta_i\theta_j[\left(A_{im} + B_{im}K_{ml}\right)\hat{x}(t) + \tilde{B}_{im}L_{jm}\left(\bar{y}(t) - C_m\hat{x}(t-\rho(t))\right)] \tag{23}$$

with $\tilde{B}_{im} = I - B_{im}\left(G_mB_{im}\right)^{-1}G_m$.

3.2 Finite-time Reachability Analysis

In the part, within a given limited time $[0,T]$, the SMC law $u(t)$ is designed to compel trajectories of the system into the sliding surface $s(t) = 0$ in a finite interval $[0,T^*]$, and ensures that they stay on the sliding surface for the rest of time $[T^*,T]$. For the purpose, the following SMC law is developed

$$u(t) = \sum_{i=1}^{v}\sum_{j=1}^{v} \eta_i\theta_j[K_{ml}\hat{x}(t) - f_m(\hat{x}(t),t) - \left(G_mB_{im}\right)^{-1} G_mL_{jm}(\bar{y}(t) - \hat{y}(t-\rho(t))) - \partial(t)\,\mathrm{sgn}(s(t))] \tag{24}$$

with $\breve{\pi}_{mn} \triangleq E[\pi_{mn}(\hbar)] \triangleq \int_0^\infty \pi_{mn}(\hbar)\S_m(\hbar)dh$, $\S_m(\hbar)$ represents the probability density function(PDF) of sojourn time $\hbar$ that stays at mode m.

Theorem 3.1. *For S-MJSs (2), the SMC law (24) enables the trajectories of the system to be compelled into the sliding surface $s(t) = 0$ in the limited timespan $[0, T^*]$ $(T^* < T)$ and stay on there in $[T^*, T]$ in mean square sense, wherein $\partial(t)$ in the sliding mode control law (24) satisfies*

$$\partial(t) \geq \frac{\left\| {B_{im}}^T \hat{x}(0) \right\|}{T\lambda_{min}\left(B_{im}^T B_{im}\right)} \tag{25}$$

Proof: Consider the Lyapunov function with respect to any $t \in [0, T]$

$$V_1(s(t), m, l, t) = \frac{1}{2} s^T(t)s(t) \tag{26}$$

To facilitate the expression, let $V_1(s(t), m, l, t) \triangleq V_1(t)$ whose infinitesimal operator is obtained:

$$\begin{aligned}
\Gamma V_1(t) =& s^T(t)\dot{s}(t) \\
=& s^T[\sum_{i=1}^{v}\sum_{j=1}^{v}\eta_i\theta_j[G_m B_{im}(K_{ml}\hat{x}(t) - (G_m B_{im})^{-1}G_m L_{jm}(\bar{y}(t) - \hat{y}(t-\rho(t))) \\
& - f_m(\hat{x}(t), t) - \partial(t)sgn(s(t))) - G_m B_{im}K_{ml}\hat{x}(t) + G_m L_{jm}(\bar{y}(t) - \hat{y}(t-\rho(t))) \\
& + G_m B_{im} f_m(\hat{x}(t), t)]] \\
=& - s^T(t)B_{im}^T B_{im}\partial(t)\,\mathrm{sgn}(s(t)) \\
\leq& - \partial(t)\lambda_{\min}\left(B_{im}^T B_{im}\right)\|s(t)\|_1 \\
\leq& - \partial(t)\lambda_{\min}\left(B_{im}^T B_{im}\right)\|s(t)\|_2
\end{aligned} \tag{27}$$

Besides,one has

$$\Gamma V_1(t) \leq -\frac{\partial(t)\,\mathrm{sgn}(s(t))}{\Bbbk}\sqrt{V_1(t)} \tag{28}$$

With

$$\Bbbk = \frac{1}{\sqrt{2}\lambda_{\min}\left(B_{im}^T B_{im}\right)} \tag{29}$$

From (28) and (29),we can get that T* satisfies

$$T^* \leq \frac{\left\| B_{im}^T \hat{x}(0) \right\|_2}{\partial(t)\lambda_{\min}\left(B_{im}^T B_{im}\right)} \tag{30}$$

Therefore, in a limited timespan $[0, T]$, the trajectories of S-MJSs (2) is to be compelled into the sliding surface (20) within limited time $T^*(T^* < T)$, and maintained there during the rest of time $[T^*, T]$, the proof is thus accomplished.

Remark 3.1. *As you can see from the certification process presented above, the parameter $\partial(t)$ in the SMC law (24) is significant and can decide the arrival time T^*. Based on (30), when the value of $\partial(t)$ is higher, the time to the arrival stage is shorter.*

Remark 3.2. *For finite-time sliding mode control, what makes it unique is that it is analyzed in pieces containing arrival stage $[0, T^*]$, with sliding mode movement stage $[T^*, T]$. The trajectories of the system will be actuated to the sliding surface $s(t) = 0$ within a limited time T^*, which has been proved in **Theorem 3.1**. Afterwards, the goal is to prove that the CLS is mean-square finite-time bounded along with the sliding surface in $[0, T]$.*

3.3 Finite-time Boundedness in $[0, T^*]$

During the subsection, the trajectories of the system are at the external side of the sliding surface within the arrival phase $[0, T^*]$, which means $s(t) \neq 0$. By incorporating (24) and (14), the CLS can be reprofiled as:

$$\begin{cases} \dot{\hat{x}}(t) = \sum\limits_{i=1}^{v}\sum\limits_{j=1}^{v} \eta_i\theta_j[(A_{im} + B_{im}K_{ml})\,\hat{x}(t) + \tilde{B}_m L_{jm}\left(\bar{y}(t) - C_m\hat{x}(t-\rho(t)) - B_{im}\bar{\partial}(t)\right)] \\ \dot{\tilde{x}}(t) = \sum\limits_{i=1}^{v}\sum\limits_{j=1}^{v} \eta_i\theta_j[A_{im}\tilde{x}(t) - L_{jm}C_m\tilde{x}(t-\rho(t)) + \lambda(t_k h)L_{jm}e_k(t) - \lambda(t_k h)L_{jm}Q(y(t_k h + \varepsilon h)) \\ +L_{jm}C_m x(t-\rho(t))] + \bar{w}(t) \end{cases} \tag{31}$$

where $\bar{\partial}(t) = \partial(t)\,\mathrm{sgn}(s(t))$

Then, the FTB issue of the system (31) is to be researched within the timespan $[0, T^*]$.

Theorem 3.2. *With respect to the positive scalars ξ_m, ξ_{1m}, and k_j satisfying $\theta_j - k_j\eta_j \geq 0$ $(k_j \in (0,1))$, $\forall m \in N_1$, the system (31) is finite-time boundedness about $\left(c_1, c^*, [0,T^*], \mathbb{W}, \Omega_{[0,T],\ell}\right)$ in reaching stage $[0,T^*]$, if there are positive definite matrices $P_{um}, Q_{um}, Q_u, u = 1,2$, and $\Lambda_i = \Lambda_i^T$ with appropriate dimensions satisfying*

$$\Theta_{ij}^* - \Lambda_i < 0 \tag{32}$$

$$k_i\Theta_{ii}^* - (1-k_i)\Lambda_i < 0 \tag{33}$$

$$k_j\Theta_{ij}^* + (1-k_j)\Lambda_i + k_i\Theta_{ji}^* + (1-k_i)\Lambda_j < 0 \tag{34}$$

$$c_1 < c^* < c_2 \tag{35}$$

$$\frac{c_1\Psi + \ell\xi_m + \xi_m\left[\bar{\partial}^2(t) + \bar{y}^2(t) + x^2(t-\rho(t)) + Q^2(y(t-\rho(t))) + Q^2(y(t_k h + \varepsilon h))\right]T^*}{\underline{\propto}_{P_{2m}}} < e^{-\xi_m T^*}c^* \tag{36}$$

$$\sum_{n=1}^{M_1}\breve{\pi}_{mn}Q_{1n} \leq Q_1, \sum_{n-1}^{M_1}\breve{\pi}_{mn}Q_{2n} \leq Q_2 \tag{37}$$

where

$$\Theta_{ij}^* = \begin{bmatrix} V_{11m}^{(1)} & 0 & 0 & 0 & V_{15m}^{(1)} & 0 & 0 & V_{18m}^{(1)} & V_{19m}^{(1)} & V_{110m}^{(1)} \\ * & -(1-g)Q_{1m} & 0 & 0 & 0 & 0 & 0 & 0 & 0 & V_{210m}^{(1)} \\ * & * & V_{33m}^{(1)} & V_{34m}^{(1)} & 0 & 0 & V_{37m}^{(1)} & 0 & 0 & V_{310m}^{(1)} \\ * & * & * & -(1-g)Q_{2m} & 0 & 0 & 0 & 0 & 0 & 0 \\ * & * & * & * & -\Phi_m & 0 & 0 & 0 & 0 & 0 \\ * & * & * & * & * & \alpha_m\Phi_m - \xi_m I & 0 & 0 & 0 & 0 \\ * & * & * & * & * & * & -\xi_m I & 0 & 0 & 0 \\ * & * & * & * & * & * & * & -\xi_m I & 0 & 0 \\ * & * & * & * & * & * & * & * & -\xi_m I & 0 \\ * & * & * & * & * & * & * & * & * & V_{1010m}^{(1)} \end{bmatrix}$$

$V_{11m}^{(1)} = \sum\limits_{n=1}^{M_1}\breve{\pi}_{mn}P_{1n} + Q_{1m} + \bar{\rho}Q_1 - \xi_m P_{1m}, V_{15m}^{(1)} = \bar{\lambda}P_{1m}L_{jm},$
$V_{18m}^{(1)} = P_{1m}L_{jm}C_m, V_{19m}^{(1)} = -\bar{\lambda}P_{1m}L_{jm},$
$V_{110m}^{(1)} = \begin{bmatrix} P_{1m} & 0 & P_{1m} & A_{im}^T \end{bmatrix}$
$V_{210m}^{(1)} = \begin{bmatrix} 0 & 0 & 0 & -C_m^T L_{jm}^T \end{bmatrix}$
$V_{33m}^{(1)} = \sum\limits_{n=1}^{M_1}\breve{\pi}_{mn}P_{2n} + Q_{2m} + \bar{\rho}Q_2 - \xi_m P_{2m} + P_{2m}A_{im}^T + A_{im}^T P_{2m} + P_{2m}\sum\limits_{l=1}^{M_2}\hat{\pi}_{ml}B_{im}K_{ml} + \sum\limits_{l=1}^{M_2}\hat{\pi}_{ml}K_{ml}^T B_{im}^T P_{2m}$
$V_{34m}^{(1)} = -P_{2m}\tilde{B}_m L_{jm}C_m, V_{37m}^{(1)} = P_{2m}\tilde{B}_m L_{jm}$
$V_{310m}^{(1)} = \begin{bmatrix} 0 & -P_{2m}B_{im} & 0 & 0 \end{bmatrix}$

$$V_{1010m}^{(1)} = -diag\left[\xi_m I \quad \xi_m I \quad \xi_{1m}^{-1} I \quad \xi_{1m} I\right]$$
$$\bar{\alpha}_{P_{1m}} = \max_{m\in N_1}\left(\lambda_{max}\left(\mathbb{W}^{-\frac{1}{2}} P_{1m}\mathbb{W}^{\frac{1}{2}}\right)\right), \bar{\alpha}_{P_{2m}} = \max_{m\in N_1}\left(\lambda_{max}\left(\mathbb{W}^{-\frac{1}{2}} P_{2m}\mathbb{W}^{\frac{1}{2}}\right)\right),$$
$$\bar{\alpha}_{Q_1} = \max_{m\in N_1}\left(\lambda_{max}\left(\mathbb{W}^{-\frac{1}{2}} Q_1\mathbb{W}^{\frac{1}{2}}\right)\right), \bar{\alpha}_{Q_2} = \max_{m\in N_1}\left(\lambda_{max}\left(\mathbb{W}^{-\frac{1}{2}} Q_2\mathbb{W}^{\frac{1}{2}}\right)\right),$$
$$\bar{\alpha}_{Q_{1m}} = \max_{m\in N_1}\left(\lambda_{max}\left(\mathbb{W}^{-\frac{1}{2}} Q_{1m}\mathbb{W}^{\frac{1}{2}}\right)\right), \bar{\alpha}_{Q_{2m}} = \max_{m\in N_1}\left(\lambda_{max}\left(\mathbb{W}^{-\frac{1}{2}} Q_{2m}\mathbb{W}^{\frac{1}{2}}\right)\right),$$
$$\underline{\alpha}_{P_{2m}} = \min_{m\in N_1}\left(\lambda_{max}\left(\mathbb{W}^{-\frac{1}{2}} P_{2m}\mathbb{W}^{\frac{1}{2}}\right)\right), \Psi = \bar{\alpha}_{P_{1m}} + \bar{\alpha}_{P_{2m}} + g\bar{\alpha}_{Q_{1m}} + \tfrac{1}{2}g^2\bar{\alpha}_{Q_1} + \tfrac{1}{2}g^2\bar{\alpha}_{Q_2}$$

Proof: Select the Lyapunov function:

$$\begin{aligned} V_2(t) &= \tilde{x}^T(t)P_{1m}\tilde{x}(t) + \int_{t-\rho(t)}^{t}\tilde{x}^T(k)Q_{1m}\tilde{x}(k)dk + \int_{-\bar{\rho}}^{0}\int_{t+q}^{t}\tilde{x}^T(k)Q_1\tilde{x}(k)dkdq \\ &+\hat{x}(t)P_{2m}\hat{x}(t) + \int_{t-\rho(t)}^{t}\hat{x}^T(k)Q_2\hat{x}(k)dk + \int_{-\bar{\rho}}^{0}\int_{t+q}^{t}\hat{x}^T(k)Q_2\hat{x}(k)dkdq \end{aligned} \tag{38}$$

the weak infinitesimal generator of $V_2(t)$ is given:

$$\begin{aligned} \Gamma V_2(t) &= 2\tilde{x}^T(t)P_{1m}\dot{\tilde{x}}(t) + \tilde{x}^T(t)(\sum_{n=1}^{M_1}\breve{\pi}_{mn}P_{1n})\tilde{x}(t) + \tilde{x}^T(t)Q_{1m}\tilde{x}(t) - (1-\dot{\rho}(t))\tilde{x}^T(t-\rho(t))Q_{1m}\tilde{x}(t-\rho(t)) \\ &+\int_{t-\rho(t)}^{t}\tilde{x}^T(k)(\sum_{n=1}^{M_1}\breve{\pi}_{mn}Q_{1n})\tilde{x}(k)dk + \bar{\rho}\tilde{x}^T(t)Q_1\tilde{x}(t) - \int_{t-\bar{\rho}}^{t}\tilde{x}^T(k)Q_1\tilde{x}(k)dk + 2\hat{x}^T(t)P_{2m}\dot{\hat{x}}(t) \\ &+\hat{x}^T(t)(\sum_{n=1}^{M_1}\breve{\pi}_{mn}P_{2n})\hat{x}(t) + \hat{x}^T(t)Q_{2m}\hat{x}(t) - (1-\dot{\rho}(t))\hat{x}^T(t-\rho(t))Q_{2m}\hat{x}(t-\rho(t)) + \bar{\rho}\hat{x}^T(t)Q_2\hat{x}(t) \\ &+\int_{t-\rho(t)}^{t}\hat{x}^T(k)(\sum_{n=1}^{M_1}\breve{\pi}_{mn}Q_{2n})\hat{x}(k)dk - \int_{t-\bar{\rho}}^{t}\hat{x}^T(k)Q_2\hat{x}(k)dk \\ &= 2\tilde{x}^T(t)P_{1m}\{\sum_{i=1}^{v}\sum_{j=1}^{v}\eta_i\theta_j[A_{im}\tilde{x}(t) - L_{jm}C_m\tilde{x}(t-\rho(t)) + \bar{\lambda}L_{jm}e_k(t) - \bar{\lambda}L_{jm}Q(y(t_kh+\varepsilon h)) \\ &+L_{jm}C_mx(t-\rho(t))]\} + 2\tilde{x}^T(t)P_{1m}\bar{w}(t) - (1-\dot{\rho}(t))\tilde{x}^T(t-\rho(t))Q_{1m}\tilde{x}(t-\rho(t)) \\ &+\tilde{x}^T(t)(\sum_{n=1}^{M_1}\breve{\pi}_{mn}P_{1n})\tilde{x}(t) + \tilde{x}^T(t)Q_{1m}\tilde{x}(t) + \int_{t-\rho(t)}^{t}\tilde{x}^T(k)(\sum_{n=1}^{M_1}\breve{\pi}_{mn}Q_{1n})\tilde{x}(k)dk \\ &+\bar{\rho}\tilde{x}^T(t)Q_1\tilde{x}(t) - \int_{t-\bar{\rho}}^{t}\tilde{x}^T(k)Q_1\tilde{x}(k)dk - \int_{t-\bar{\rho}}^{t}\hat{x}^T(k)Q_2\hat{x}(k)dk + \bar{\rho}\hat{x}^T(t)Q_2\hat{x}(t) \\ &+2\hat{x}^T(t)P_{2m}\{\sum_{i=1}^{v}\sum_{j=1}^{v}\eta_i\theta_j[A_{im}\hat{x}(t) + \sum_{l=1}^{M_2}\hat{\pi}_{ml}B_{im}K_{ml}\hat{x}(t) + \tilde{B}_mL_{jm}(\bar{y}(t) - C_m\hat{x}(t-\rho(t))) \\ &-B_{im}\bar{\partial}(t)]\} - (1-\dot{\rho}(t))\hat{x}^T(t-\rho(t))Q_{2m}\hat{x}(t-\rho(t)) + \hat{x}^T(t)(\sum_{n=1}^{M_1}\breve{\pi}_{mn}P_{2n})\hat{x}(t) \\ &+\hat{x}^T(t)Q_{2m}\hat{x}(t) + \int_{t-\rho(t)}^{t}\hat{x}^T(k)(\sum_{n=1}^{M_1}\breve{\pi}_{mn}Q_{2n})\hat{x}(k)dk \end{aligned}$$

In line with **Lemma 2.1**, for positive scalars ξ_{1m}, one can get that.

$$\begin{aligned} &2\tilde{x}^T(t)P_{1m}[A_{im}\tilde{x}(t) - L_{jm}C_m\tilde{x}(t-\rho(t))] \le \xi_{1m}\tilde{x}^T(t)P_{1m}P_{1m}\tilde{x}(t) \\ &+\xi_{1m}^{-1}[\tilde{x}^T(t)A_{im}^T - \tilde{x}^T(t-\rho(t))C_m^TL_{jm}^T][A_{im}\tilde{x}(t) - L_{jm}C_m\tilde{x}(t-\rho(t))] \end{aligned} \tag{39}$$

Define an additional function:

$$\begin{aligned} &H_1(t) = \Gamma V_2(t) - \xi_m V_2(t) - \xi_m\bar{w}^T(t)\bar{w}(t) - \xi_m\bar{\partial}^T(t)\bar{\partial}(t) - \xi_m\bar{y}^T(t)\bar{y}(t) \\ &-\xi_m x^T(t-\rho(t))x(t-\rho(t)) - \xi_m Q^T(y(t-\rho(t)))Q(y(t-\rho(t))) - \xi_m Q^T(y(t_kh+\varepsilon h))Q(y(t_kh+\varepsilon h)) \end{aligned} \tag{40}$$

In accordance with **Appendix A**, we can readily obtain that $H_1(t) < 0$ which means that

$$\begin{aligned} &\Gamma V_2(t) \le \xi_m V_2(t) + \xi_m\bar{w}^T(t)\bar{w}(t) + \xi_m\bar{\partial}^T(t)\bar{\partial}(t) + \xi_m\bar{y}^T(t)\bar{y}(t) \\ &+\xi_m x^T(t-\rho(t))x(t-\rho(t)) + \xi_m Q^T(y(t-\rho(t)))Q(y(t-\rho(t))) + \xi_m Q^T(y(t_kh+\varepsilon h))Q(y(t_kh+\varepsilon h)) \end{aligned} \tag{41}$$

Then, the both sides of the inequation (41) are multiplied by $e^{-\xi_m t}$ and integrated range from 0 to t with $t \in [0, T^*]$ lead to

$$\begin{array}{l} e^{-\xi_m} E\left\{V_2(t)\right\} < E\left\{V_2(0)\right\} + \xi_m \int_0^t e^{-\xi_m k} \bar{w}^T(k)\bar{w}(k)dk + \xi_m \int_0^t e^{-\xi_m k} \bar{\partial}^T(k)\bar{\partial}(k)dk \\ +\xi_m \int_0^t e^{-\xi_m k} \bar{y}^T(k)\bar{y}(k)dk + \xi_m \int_0^t e^{-\xi_m k} x^T(k-\rho(k))x(k-\rho(k))dk \\ +\xi_m \int_0^t e^{-\xi_m k} Q^T(y(k-\rho(k)))Q(y(k-\rho(k)))dk + \xi_m \int_0^t e^{-\xi_m k} Q^T(y(t_k h+\varepsilon h))Q(y(t_k h+\varepsilon h))dk \end{array} \tag{42}$$

As can be derived from the inequality (42) that

$$E\left\{V_2(0)\right\} \leq \Psi \times \sup_{-\bar{\rho} \leq s \leq 0} \left\{\tilde{x}^T(s) W \tilde{x}(s), \hat{x}^T(s) W \hat{x}(s)\right\} \tag{43}$$

According to **Definition 2.1**, we can get:

$$\Gamma V_2(0) \leq c_1 \Psi, where \quad \Psi = \bar{\alpha}_{P_{1m}} + \bar{\alpha}_{P_{2m}} + \bar{\rho}\bar{\alpha}_{Q_{1m}} + \bar{\rho}\bar{\alpha}_{Q_{2m}} + \frac{1}{2}\bar{\rho}^2 \bar{\alpha}_{Q_1} + \frac{1}{2}\bar{\rho}^2 \bar{\alpha}_{Q_2}$$

Further, combined with **Assumption 2.1**, there is

$$\begin{array}{rl} E\left\{V_2(t)\right\} < & [c_1\Psi + \xi_m \ell + \xi_m \bar{\partial}^2(t) T^* + \xi_m \bar{y}^2(t) T^* + \xi_m x^2\left(t-\rho(t)\right) T^\star + \xi_m Q^2(y(t-\rho(t))) T^* \\ & + \xi_m Q^2(y(t_k h+\varepsilon h)) T^*] e^{\xi_m t} \end{array} \tag{44}$$

Additionally, in combination with (38), we get that

$$E\left\{V_2(t)\right\} \geq E\left\{\hat{x}^T(t) P_{2m} \hat{x}(t)\right\} \geq \underline{\alpha}_{P_{2m}} E\left\{\hat{x}^T(t) W \hat{x}(t)\right\} \tag{45}$$

In light of (44) with (45), one can obtain that

$$E\left\{\hat{x}^T(t) W \hat{x}(t)\right\} \leq \frac{c_1\Psi + \ell\xi_m + \xi_m\left[\bar{\partial}^2(t) + \bar{y}^2(t) + x^2(t-\rho(t)) + Q^2 y(t-\rho(t)) + Q^2(y(t_k h+\varepsilon h))\right] T^*}{e^{-\xi_m T^*} \underline{\alpha}_{P_{2m}}} \tag{46}$$

Moreover, there exists a scalar c^* meeting (35) so that

$$\frac{c_1\Psi + \ell\xi_m + \xi_m\left[\bar{\partial}^2(t) + \bar{y}^2(t) + x^2(t-\rho(t)) + Q^2 y(t-\rho(t)) + Q^2(y(t_k h+\varepsilon h))\right] T^*}{\underline{\alpha}_{P_{2m}}} \leq e^{-\xi_m T^*} c^* \tag{47}$$

Based on (46), we can get that $E\left\{\hat{x}^T(t) W \hat{x}(t)\right\} \leq c^*$ with $t \in [0, T^*]$. Accordingly, the system (31) is finite-time boundedness.

Next, the finite-time boundedness problem of the system (15) under the equivalence of SMC law (22) will be studied in the timespan $[T^*, T]$.

Theorem 3.3. *For the positive scalars ξ_m, ξ_{1m},and k_j satisfying $\theta_j - k_j\eta_j \geq 0$ $(k_j \in (0,1))$, $\forall m \in N_1$,the system (23) is finite-time boundedness about $\left(c^*, c_2, [T^*, T], \mathbb{W}, \Omega_{[0,T],\ell}\right)$,if there are positive definite matrices $P_{um}, Q_{um}, Q_u, u = 1, 2$, and $\tilde{\Lambda}_i = \tilde{\Lambda}_i^T$ with appropriate dimensions satisfying*

$$\tilde{\Theta}_{ij}^* - \tilde{\Lambda}_i < 0 \tag{48}$$

$$k_i \tilde{\Theta}_{ii}^* - (1-k_i)\tilde{\Lambda}_i < 0 \tag{49}$$

$$k_j \tilde{\Theta}_{ij}^* + (1-k_j)\tilde{\Lambda}_i + k_i \tilde{\Theta}_{ji}^* + (1-k_i)\tilde{\Lambda}_j < 0 \tag{50}$$

$$c_1 < c^* < c_2 \tag{51}$$

$$\frac{c_1\Psi + \ell\xi_m + \xi_m\left[\bar{y}^2(t) + x^2(t-\rho(t)) + Q^2(y(t-\rho(t))) + Q^2(y(t_k h+\varepsilon h))\right] T}{\underline{\alpha}_{P_{2m}}} < e^{-\xi_m T} c_2 \tag{52}$$

$$\sum_{n=1}^{M_1} \breve{\pi}_{mn} Q_{1n} \leq Q_1, \sum_{n-1}^{M_1} \breve{\pi}_{mn} Q_{2n} \leq Q_2 \tag{53}$$

where

$$\tilde{\Theta}_{ij}^{*}=\begin{bmatrix} V_{11m}^{(2)} & 0 & 0 & 0 & V_{15m}^{(2)} & 0 & 0 & V_{18m}^{(2)} & V_{19m}^{(2)} & V_{110m}^{(2)} \\ * & -(1-g)Q_{1m} & 0 & 0 & 0 & 0 & 0 & 0 & 0 & 0 \\ * & * & V_{33m}^{(1)} & V_{34m}^{(1)} & 0 & 0 & V_{37m}^{(1)} & 0 & 0 & 0 \\ * & * & * & -(1-g)Q_{2m} & 0 & 0 & 0 & 0 & 0 & 0 \\ * & * & * & * & -\Phi_m & 0 & 0 & 0 & 0 & 0 \\ * & * & * & * & * & \alpha_m\Phi_m-\xi_m I & 0 & 0 & 0 & 0 \\ * & * & * & * & * & * & -\xi_m I & 0 & 0 & 0 \\ * & * & * & * & * & * & * & -\xi_m I & 0 & 0 \\ * & * & * & * & * & * & * & * & -\xi_m I & 0 \\ * & * & * & * & * & * & * & * & * & V_{1010m}^{(2)} \end{bmatrix}$$

$V_{11m}^{(2)}=V_{11m}^{(1)}, V_{15m}^{(2)}=V_{15m}^{(1)}, V_{18m}^{(2)}=V_{18m}^{(1)}, V_{19m}^{(2)}=V_{19m}^{(1)}, V_{110m}^{(2)}=\begin{bmatrix}P_{1m} & P_{1m} & A_{im}^{T}\end{bmatrix}$,
$V_{33m}^{(2)}=V_{33m}^{(1)}, V_{34m}^{(2)}=V_{34m}^{(1)}, V_{37m}^{(2)}=V_{37m}^{(1)}, V_{210m}^{(2)}=\begin{bmatrix}0 & 0 & -C_m^T L_{jm}^T,\end{bmatrix}$,
$V_{1010m}^{(2)}=-diag\begin{bmatrix}\xi_m I & \xi_{1m}^{-1} I & \xi_{1m} I\end{bmatrix}$.

Proof: Pick the Lyapunov function $V_3(t)=V_2(t)$.

In combination with (23), define the additional function:

$$\begin{aligned} &H_2(t)=\Gamma V_3(t)-\xi_m V_3(t)-\xi_m\bar{w}^T(t)\bar{w}(t)-\xi_m\bar{y}^T(t)\bar{y}(t)-\xi_m x^T(t-\rho(t))x(t-\rho(t)) \\ &-\xi_m Q^T(y(t-\rho(t)))Q(y(t-\rho(t)))-\xi_m Q^T(y(t_k h+\varepsilon h)Q(y(t_k h+\varepsilon h)) \end{aligned} \tag{54}$$

In accordance with **Appendix B**, we can readily obtain that $H_2(t)<0$ which means that

$$\begin{aligned} &\Gamma V_3(t)\leq\xi_m V_3(t)+\xi_m\bar{w}^T(t)\bar{w}(t)+\xi_m\bar{y}^T(t)\bar{y}(t)+\xi_m x^T(t-\rho(t))x(t-\rho(t)) \\ &+\xi_m Q^T(y(t-\rho(t)))Q(y(t-\rho(t)))+\xi_m Q^T(y(t_k h+\varepsilon h))Q(y(t_k h+\varepsilon h)) \end{aligned} \tag{55}$$

Next, the latter part of the certification equates to **Theorem 3.2**, with regard to $t\in[T^*,T]$, we have

$$\begin{aligned} &e^{-\xi_m t}E\left\{V_3(t)\right\}<E\left\{V_3\left(T^*\right)\right\}+\xi_m\int_0^t e^{-\xi_m k}\bar{w}^T(k)\bar{w}(k)dk+\xi_m\int_0^t e^{-\xi_m k}\bar{y}^T(k)\bar{y}(k)dk \\ &+\xi_m\int_0^t e^{-\xi_m k}x^T(k-\rho(k))x(k-\rho(k))dk+\xi_m\int_0^t e^{-\xi_m k}Q^T(y(k-\rho(k)))Q(y(k-\rho(k)))dk \\ &+\xi_m\int_0^t e^{-\xi_m k}Q^T(y(t_k h+\varepsilon h)Q(y(t_k h+\varepsilon h)) \\ &<c^*\Psi+\ell\xi_m+\xi_m\left[\bar{y}^2(t)+x^2(t-\rho(t))+Q^2(y(t-\rho(t)))+Q^2(y(t_k h+\varepsilon h))\right]T \end{aligned} \tag{56}$$

Consequently, it can be deduced that

$$E\left\{V_3(t)\right\}\geq E\left\{\hat{x}^T(t)P_{2m}\hat{x}(t)\right\}\geq\varpropto_{P_{2m}}E\left\{\hat{x}^T(t)W\hat{x}(t)\right\} \tag{57}$$

In light of (56) with (57), one gets that

$$\frac{c^*\Psi+\ell\xi_m+\xi_m\left[\bar{y}^2(t)+x^2(t-\rho(t))+Q^2y(t-\rho(t))+Q^2(y(t_k h+\varepsilon h))\right]T^*}{\varpropto_{P_{2m}}}\leq e^{-\xi_m T}c_2 \tag{58}$$

One gets from the above that $E\left\{\hat{x}^T(t)W\hat{x}(t)\right\}\leq c_2$ with respect to $t\in[T^*,T]$. Therefore, the system (23) is finite-time boundedness.

Theorem 3.4. *For given positive scalars $\xi_{1m},\xi_m,\gamma_{\bar{P}_{1m}},\gamma_{\bar{P}_{2m}},\gamma_{Q_{1m}},\gamma_{Q_{2m}}\gamma_{\bar{Q}_1},\gamma_{\bar{Q}_2}$, and k_j satisfying $\theta_j-k_j\eta_j\geq 0$ $(k_j\in(0,1))$, $\forall m\in N_1$, the system is finite-time boundedness within $[0,T]$, if there are symmetric matrices $\bar{P}_{1m}>0,\bar{P}_{2m}>0,Q_{1m}>0,Q_{2m}>0,\bar{Q}_1>0,\bar{Q}_2>0,\mathbb{W}>0$ and $\bar{\Lambda}_i=\bar{\Lambda}_i^T$, $\mathbb{K}_{ml}$ with appropriate dimension, such that*

$$\bar{\Theta}_{ij}^{*}-\bar{\Lambda}_i<0 \tag{59}$$

$$k_i\bar{\Theta}_{ii}^{*}-(1-k_i)\bar{\Lambda}_i<0 \tag{60}$$

$$k_j\bar{\Theta}_{ij}^{*}+(1-k_j)\bar{\Lambda}_i+k_i\bar{\Theta}_{ji}^{*}+(1-k_i)\bar{\Lambda}_j<0 \tag{61}$$

$$c_1<c^{*}<c_2 \tag{62}$$

$$\begin{cases}\gamma_{\bar{P}_{1m}}\mathbb{W}^{-1}<\bar{P}_{1m}<2\mathbb{W}^{-1}\\ \gamma_{\bar{P}_{2m}}\mathbb{W}^{-1}<\bar{P}_{2m}<2\mathbb{W}^{-1}\\ \gamma_{Q_{1m}}\mathbb{W}^{-1}<Q_{1m}<2\mathbb{W}^{-1}\\ \gamma_{Q_{2m}}\mathbb{W}^{-1}<Q_{2m}<2\mathbb{W}^{-1}\\ \gamma_{\bar{Q}_1}\mathbb{W}^{-1}<\bar{Q}_1<2\mathbb{W}^{-1}\\ \gamma_{\bar{Q}_2}\mathbb{W}^{-1}<\bar{Q}_2<2\mathbb{W}^{-1}\end{cases} \tag{63}$$

$$\begin{bmatrix}\Sigma_{11} & \Sigma_{12}\\ * & \Sigma_{22}\end{bmatrix}<0 \tag{64}$$

$$\begin{bmatrix}\bar{\Sigma}_{11} & \bar{\Sigma}_{12}\\ * & \bar{\Sigma}_{22}\end{bmatrix}<0 \tag{65}$$

where

$$\bar{\Theta}_{ij}^{*}=\begin{bmatrix}\mathbb{H}_1 & \mathbb{H}_2 & \mathbb{H}_3 & \mathbb{H}_4 & \mathbb{H}_5 & \mathbb{H}_6 & \mathbb{H}_7 & \mathbb{H}_8 & \mathbb{H}_9 & \mathbb{H}_{10} & \mathbb{H}_{11} & \mathbb{H}_{12}\end{bmatrix}$$

$$\mathbb{H}_1=\begin{bmatrix}V_{11m}^{(3)\,T} & 0 & 0 & 0 & V_{15m}^{(3)} & 0 & 0 & V_{18m}^{(3)} & V_{19m}^{(3)} & V_{110m}^{(3)} & V_{111m}^{(3)} & 0\end{bmatrix}^T$$

$$\mathbb{H}_2=\begin{bmatrix}0 & -(1-g)Q_{1m} & 0 & 0 & 0 & 0 & 0 & 0 & 0 & V_{210m}^{(3)} & 0 & 0\end{bmatrix}^T$$

$$\mathbb{H}_3=\begin{bmatrix}0 & 0 & V_{33m}^{(3)\,T} & V_{34m}^{(3)} & 0 & 0 & V_{37m}^{(3)} & 0 & 0 & V_{310m}^{(3)} & 0 & V_{312m}^{(3)}\end{bmatrix}^T$$

$$\mathbb{H}_4=\begin{bmatrix}0 & 0 & V_{34m}^{(3)\,T} & -(1-g)Q_{2m} & 0 & 0 & 0 & 0 & 0 & 0 & 0 & 0\end{bmatrix}^T$$

$$\mathbb{H}_5=\begin{bmatrix}V_{15m}^{(3)\,T} & 0 & 0 & 0 & -\Phi_m & 0 & 0 & 0 & 0 & 0 & 0 & 0\end{bmatrix}^T$$

$$\mathbb{H}_6=\begin{bmatrix}0 & 0 & 0 & 0 & 0 & \alpha_m\Phi_m-\xi_m I & 0 & 0 & 0 & 0 & 0 & 0\end{bmatrix}^T$$

$$\mathbb{H}_7=\begin{bmatrix}0 & 0 & V_{37m}^{(3)\,T} & 0 & 0 & 0 & -\xi_m I & 0 & 0 & 0 & 0 & 0\end{bmatrix}^T$$

$$\mathbb{H}_8=\begin{bmatrix}V_{18m}^{(3)\,T} & 0 & 0 & 0 & 0 & 0 & 0 & -\xi_m I & 0 & 0 & 0 & 0\end{bmatrix}^T$$

$$\mathbb{H}_9=\begin{bmatrix}V_{19m}^{(3)\,T} & 0 & 0 & 0 & 0 & 0 & 0 & 0 & -\xi_m I & 0 & 0 & 0 & 0\end{bmatrix}^T$$

$$\mathbb{H}_{10}=\begin{bmatrix}V_{110m}^{(3)\,T} & V_{210m}^{(3)\,T} & V_{310m}^{(3)\,T} & 0 & 0 & 0 & 0 & 0 & 0 & V_{1010m}^{(3)\,T} & 0 & 0\end{bmatrix}^T$$

$$\mathbb{H}_{11}=\begin{bmatrix}V_{111m}^{(3)\,T} & 0 & 0 & 0 & 0 & 0 & 0 & 0 & 0 & 0 & V_{1111m}^{(3)\,T} & 0\end{bmatrix}^T$$

$$\mathbb{H}_{12}=\begin{bmatrix}0 & 0 & V_{312m}^{(3)\,T} & 0 & 0 & 0 & 0 & 0 & 0 & 0 & 0 & V_{1212m}^{(3)\,T}\end{bmatrix}^T$$

$V_{11m}^{(3)}=\breve{\pi}_{mn}\bar{P}_{1m}+\bar{Q}_{1m}+g\bar{Q}_1+\xi_{1m}I-\xi_m P_{1m}, V_{15m}^{(3)}=\bar{\lambda}L_{jm},$

$V_{18m}^{(3)}=L_{jm}C_m, V_{19m}^{(3)}=-\bar{\lambda}L_{jm},$

$V_{110m}^{(3)}=\begin{bmatrix}I & 0 & \bar{P}_{1m}A_{im}^{T}\end{bmatrix},$

$V_{111m}^{(3)}=\begin{bmatrix}\sqrt{\breve{\pi}_{m1}}\bar{P}_{1m} & \cdots & \sqrt{\breve{\pi}_{m(m-1)}}\bar{P}_{1m} & \sqrt{\breve{\pi}_{m(m+1)}}\bar{P}_{1m} & \cdots & \sqrt{\breve{\pi}_{mN_1}}\bar{P}_{1m}\end{bmatrix}$

$V_{210m}^{(3)}=\begin{bmatrix}0 & 0 & -C_m^T L_{jm}^T\end{bmatrix},$

$V_{33m}^{(3)}=\breve{\pi}_{mn}\bar{P}_{2m}+\bar{Q}_{2m}+g\bar{Q}_2+A_{im}\bar{P}_{2m}+\bar{P}_{2m}A_{im}^T+\sum_{l=1}^{M_2}\hat{\pi}_{ml}B_{im}\tilde{\mathbb{K}}_{ml}+\sum_{l=1}^{M_2}\hat{\pi}_{ml}\tilde{\mathbb{K}}_{ml}^T B_{im}^T-\xi_m\bar{P}_{2m},$

$V_{34m}^{(3)}=-\tilde{B}_{im}L_{jm}C_m, V_{37m}^{(3)}=\tilde{B}_{im}L_{jm}, V_{310m}^{(3)}=\begin{bmatrix}0 & -B_{im} & 0\end{bmatrix},$

$V_{312m}^{(3)}=\begin{bmatrix}\sqrt{\breve{\pi}_{m1}}\bar{P}_{2m} & \cdots & \sqrt{\breve{\pi}_{m(m-1)}}\bar{P}_{2m} & \sqrt{\breve{\pi}_{m(m+1)}}\bar{P}_{2m} & \cdots & \sqrt{\breve{\pi}_{mN_1}}\bar{P}_{2m}\end{bmatrix},$

$V_{1010m}^{(3)}=-diag\begin{bmatrix}\xi_m I & \xi_m I & \xi_{1m}I\end{bmatrix},$

$V_{1111m}^{(3)}=-diag\begin{bmatrix}\bar{P}_{11} & \cdots & \bar{P}_{1(m-1)} & \bar{P}_{1(m+1)} & \cdots & \bar{P}_{1N_1}\end{bmatrix},$

$V_{1212m}^{(3)} = -diag\left[\bar{P}_{21} \quad \cdots \quad \bar{P}_{2(m-1)} \quad \bar{P}_{2(m+1)} \quad \cdots \quad \bar{P}_{2N_1}\right],$
$\Sigma_{11} = -\frac{1}{2}e^{-\xi_m T}c^* + \ell_m + \xi_m\left(\partial^2(t) + \bar{y}^2(t) + x^2(t-\rho(t)) + Q^2(y(t-\rho(t))) + Q^2(y(t_k h + \varepsilon h))\right)T$
$\Sigma_{12} = \left[\sqrt{c}_1 \quad \sqrt{c}_1 \quad \sqrt{c}_1 \quad \sqrt{c}_1 \quad \sqrt{c}_1 \quad \sqrt{c}_1\right],$
$\Sigma_{22} = -diag\left[\gamma_{\bar{P}_{1m}} \quad \gamma_{\bar{P}_{2m}} \quad g^{-1}\gamma_{Q_{1m}} \quad g^{-1}\gamma_{Q_{2m}} \quad g^{-2}\gamma_{\bar{Q}_1} \quad g^{-2}\gamma_{\bar{Q}_2}\right],$
$\bar{\Sigma}_{11} = -\frac{1}{2}e^{-\xi_m T}c_2 + \ell\xi_m + \xi_m\left(\bar{y}^2(t) + x^2(t-\rho(t)) + Q^2(y(t-\rho(t))) + Q^2(y(t_k h + \varepsilon h))\right)T$
$\bar{\Sigma}_{12} = \left[\sqrt{c^*} \quad \sqrt{c^*} \quad \sqrt{c^*} \quad \sqrt{c^*} \quad \sqrt{c^*} \quad \sqrt{c^*}\right], \bar{\Sigma}_{22} = \Sigma_{22}.$

And then, gains of controller are $K_{ml} = \tilde{\mathbb{K}}_{ml}\bar{P}_{2m}^{-1}$ and gains of observer L_{jm} can be calculated by Matlab.

Proof. Define

$\bar{P}_{1m} \triangleq P_{1m}^{-1}, \bar{P}_{2m} \triangleq P_{2m}^{-1}, \bar{Q}_{1m} \triangleq P_{1m}^{-1}Q_{1m}P_{1m}^{-1}, \bar{Q}_{2m} \triangleq P_{2m}^{-1}Q_{2m}P_{2m}^{-1}, \bar{Q}_1 \triangleq P_{1m}^{-1}Q_1P_{1m}^{-1},$
$\bar{Q}_2 \triangleq P_{2m}^{-1}Q_2P_{2m}^{-1}, \tilde{\mathbb{K}}_{ml} = K_{ml}\bar{P}_{2m}, \maltese = -diag\left[P_{1m} \quad I \quad P_{2m} \quad I \quad \ldots \quad I\right].$

In accordance with (59) and Schur complement, we can get that

$$\bar{\Theta}_{ij} - \bar{\Lambda}_i < 0 \tag{66}$$

Next, pre and post-multiplying (66) ✠ and it's transpose. Afterwards, combined with Schur comlement again, the inequality (32),(48) are confirmed.

Similar to the above certification process, we can obtain that (33),(34),(49),(50) can be ensured by (60),(61).

Then,according to (63),we have

$$\begin{cases} \overline{\alpha}_{P_{1m}} < \frac{1}{\gamma_{P_{1m}}}, & \underline{\alpha}_{P_{1m}} > \frac{1}{2} \\ \overline{\alpha}_{P_{2m}} < \frac{1}{\gamma_{P_{2m}}}, & \underline{\alpha}_{P_{2m}} > \frac{1}{2} \\ \overline{\alpha}_{Q_{1m}} < \frac{1}{\gamma_{Q_{1m}}}, & \underline{\alpha}_{Q_{1m}} > \frac{1}{2} \\ \overline{\alpha}_{Q_{2m}} < \frac{1}{\gamma_{Q_{2m}}}, & \underline{\alpha}_{Q_{2m}} > \frac{1}{2} \\ \overline{\alpha}_{Q_1} < \frac{1}{\gamma_{Q_1}}, & \underline{\alpha}_{Q_1} > \frac{1}{2} \\ \overline{\alpha}_{Q_2} < \frac{1}{\gamma_{Q_2}}, & \underline{\alpha}_{Q_2} > \frac{1}{2} \end{cases}$$

According to **Theorem 3.4**, the solvable gains of controller are $K_{ml} = \tilde{\mathbb{K}}_{ml}\bar{P}_{2m}^{-1}$ and gains of observer L_{jm} can be solved by Matlab.

4 NUMERICAL EXAMPLES

In the chapter, our goal is to verify the validity of the presented control plan via a numerical instance.

Consider a two-rule interval type-II fuzzy S-MJSs and controllers both with two modes, which means $M_1 = 2, M_2 = 2$. The transition between the two models is controlled by a semi-Markov process, and the transition rate matrix below:

$$||_1(\hbar) = \begin{bmatrix} \pi_{11}(\hbar) & \pi_{12}(\hbar) \\ \pi_{21}(\hbar) & \pi_{22}(\hbar) \end{bmatrix} = \begin{bmatrix} -0.51h & 0.51h \\ 3.07h^2 & -3.07h^2 \end{bmatrix}$$

Based on the transition rate function described by the Weibull distribution, the probability density function of sojourn time is defined as $\S_m(\hbar) = \frac{c}{b^c}\hbar^{c-1}\exp[-(\frac{\hbar}{b})^c]$. When $m = 1, b = 2$ and $c = 2$, we get $\S_1(\hbar) = 0.5\hbar e^{-0.25\hbar^2}$. When $m = 2, b = 1, c = 3$, we have $\S_2(\hbar) = 3\hbar^2 e^{-\hbar^3}$. Consequently, computing mathematical expectations of transition rate function as $E\{\pi_{12}(\hbar)\} = \int_0^\infty 0.51\hbar\S_1(\hbar)d\hbar \approx 0.9040$ with $E\{\pi_{21}(\hbar)\} = \int_0^\infty 3\hbar^2\S_2(\hbar)d\hbar \approx 2.7714$, one gets

$$[\breve{\pi}_{mn}]_{m,n\in M_1} = \begin{bmatrix} -0.9040 & 0.9040 \\ 2.7714 & -2.7714 \end{bmatrix}$$

Furthermore, select the conditional probability matrix

$$||_2 = \begin{bmatrix} 0.27 & 0.73 \\ 0.38 & 0.62 \end{bmatrix}$$

The correlative system parameters are listed as follows

$A_{11} = \begin{bmatrix} -0.11 & 0.09 \\ 0.09 & -0.11 \end{bmatrix}, A_{12} = \begin{bmatrix} -0.2 & 2 \\ 1.2 & -0.7 \end{bmatrix}, A_{21} = \begin{bmatrix} -0.11 & 0.019 \\ 0.041 & -0.31 \end{bmatrix}, A_{22} = \begin{bmatrix} -0.2 & 0.7 \\ 1.1 & -0.6 \end{bmatrix}$

$B_{11} = \begin{bmatrix} -0.011 \\ 0.12 \end{bmatrix}, B_{12} = \begin{bmatrix} 0.3 \\ 0.24 \end{bmatrix}, B_{21} = \begin{bmatrix} -0.051 \\ 0.19 \end{bmatrix}, B_{22} = \begin{bmatrix} 0.11 \\ 0.05 \end{bmatrix}$

$C_1 = \begin{bmatrix} -0.2 & 0.17 \end{bmatrix}, C_2 = \begin{bmatrix} -0.4 & 0.9 \end{bmatrix}, G_1 = \begin{bmatrix} 0.15 & -0.32 \end{bmatrix}, G_2 = \begin{bmatrix} 0.23 & -0.12 \end{bmatrix}$

$D_{11} = \begin{bmatrix} 0.21 \\ 0.2 \end{bmatrix}, D_{12} = \begin{bmatrix} 0.33 \\ 0.27 \end{bmatrix}, D_{21} = \begin{bmatrix} 0.15 \\ 0.30 \end{bmatrix}, D_{22} = \begin{bmatrix} 0.27 \\ 0.09 \end{bmatrix}$

with $w(t) = 0.23sin(0.7t)$,the upper with lower membership functions:

$\underline{\eta}_1(x) = 0.85(1 - \frac{1}{1+e^{-(x_1+\frac{11}{2})/8}}), \overline{\eta}_1(x) = 0.85(1 - \frac{1}{1+e^{-(x_1+\frac{5}{2})/8}})$

$\underline{\eta}_2(x) = 1 - \underline{\eta}_1(x), \overline{\eta}_2(x) = 1 - \overline{\eta}_1(x)$

Table 1. The presented control schemes under distinct fading channels

Fading channel	K_{ml}	L_{jm}	Φ_m	Triggering number
$\bar{\lambda} = 0.8$	$K_{11} = [-15.9077, 11.4196]$	$L_{11} = [1.5734, 2.5973]^T$	$\Phi_1 = 1.1705$	17
	$K_{12} = [-10.2118, 9.2646]$	$L_{12} = [1.3352, 2.6308]^T$	$\Phi_2 = 1.3090$	
	$K_{21} = [-20.5846, 25.8407]$	$L_{21} = [1.7604, 3.2144]^T$		
	$K_{22} = [-15.3144, 27.3089]$	$L_{22} = [1.6734, 3.0831]^T$		
$\bar{\lambda} = 0.5$	$K_{11} = [-13.6621, 16.1741]$	$L_{11} = [1.4401, 3.5205]^T$	$\Phi_1 = 1.2413$	20
	$K_{12} = [-10.2803, 5.2637]$	$L_{12} = [1.4712, 3.5641]^T$	$\Phi_2 = 1.2709$	
	$K_{21} = [-13.4732, 22.3271]$	$L_{21} = [1.7134, 4.0129]^T$		
	$K_{22} = [-16.1034, 19.4407]$	$L_{22} = [1.6930, 4.0945]^T$		
$\bar{\lambda} = 0.2$	$K_{11} = [-8.3201, 27.1291]$	$L_{11} = [0.2153, 0.3021]^T$	$\Phi_1 = 1.3217$	23
	$K_{12} = [-11.4385, 18.3509]$	$L_{12} = [0.1841, 0.2703]^T$	$\Phi_1 = 1.3469$	
	$K_{21} = [-5.4328, 15.3321]$	$L_{21} = [0.1942, 0.2835]^T$		
	$K_{22} = [-7.2180, 13.7341]$	$L_{22} = [0.1731, 0.2317]^T$		

and the weighting coefficients $\underline{v}_1 = sin^2(x_1), \overline{v}_1 = 1 - sin^2(x_1)$. The actual membership functions are expressed as $\eta_1(x) = \underline{\eta}_1(x)\underline{v}_1 + \overline{\eta}_1(x)\overline{v}_1$ and $\eta_2(x) = 1 - \eta_1(x)$.

The nonlinear actuator fault signals are set as $f_1(x(t), t) = f_2(x(t), t) = 0.4sin\sqrt{x_1^2(t) + x_2^2(t)}$. The state observer (14) is desighed with the membership functions $\theta_j(\hat{x}) = 0.3\underline{\eta}_j(\hat{x}) + 0.5\overline{\eta}_j(\hat{x})(j = 1)$, and $\theta_2(\hat{x}) = 1 - \theta_1(\hat{x}(t))$. To perform the emulation, the starting location is selected as $x(0) = [-1.7, 1.7]^T, \hat{x}(0) = [0.6, -1.2]^T$.

Therefore, the parameters can be chosen as $\xi_1 = 0.3$, $\xi_2 = 0.5$, $\xi_{11} = 0.4$, $\xi_{12} = 0.25$, $k_i = 0.15$; $0.24(i = 1, 2)$, $k_j = 0.04$; $0.37(j = 1, 2)$, $\alpha_1 = 0.3$, $\alpha_2 = 0.35$, $\bar{\rho} = 0.04$, $g = 0.35$, $\psi = 0.81$, $\beta_0 = 10, c_1 = 1, c_2 = 12, \ell = 0.6, T = 10s$. For the purpose of examining the effect of the attenuation phenomenon, we also consider PET SMC influenced by distinct fading channels with $\bar{\lambda} = 0.8, 0.5, 0.2$ and the results are shown in Table 1, respectively.

The emulation results for the aforementioned examples with varied fading channels are shown in Fig.2-Fig.5 and Table 1. For simplicity, define $t_k \triangleq t_k h, \mu(t_k) \triangleq \lambda(t_k h), \bar{\mu} \triangleq \bar{\lambda}$. The trajectories of the CLS state in Fig.2-Fig.5 finally reach a stable state, remaining within a given region ($c_2 = 12$) for 0 to 10 seconds. Consequently, in line with **Definition 2.1**, the CLS is FTB with regard to $(1, 12, [0, 10], I, 0.6)$. From Fig.2 to Fig.5, the trajectories of the estimated system state are shown.

It can be seen that the observer can simulate the primitive system nicely and attain great stability. From Fig.3, we can see that the trajectories of the sliding variable can be compelled into the sliding surface $s(t) = 0$ at $t = T^*, T^* < T$ and it also depicts the SMC law. Fig 6 shows that the system modes are not in synch with the controller modes.

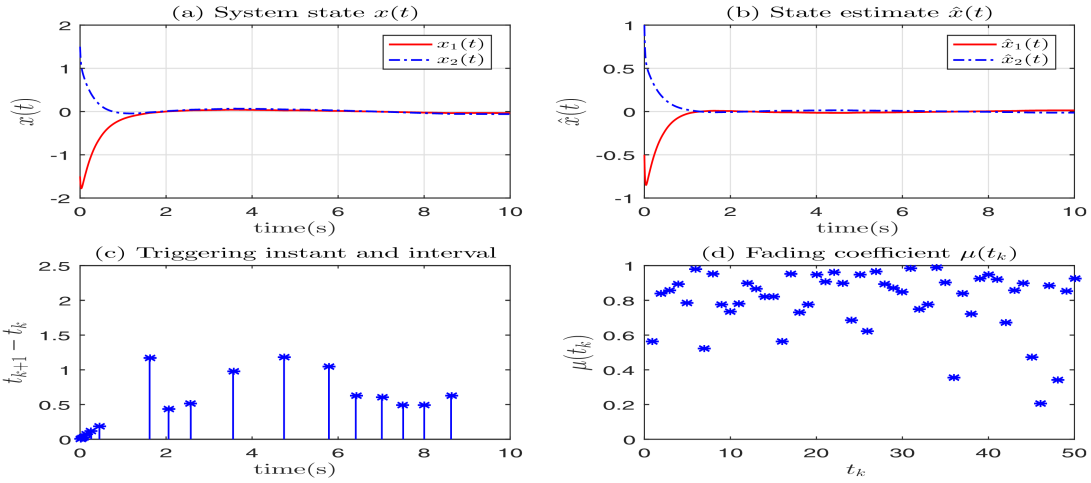

Fig. 2. States $x(t)$ and estimates $\hat{x}(t)$ with $\bar{\mu} = 0.8$.

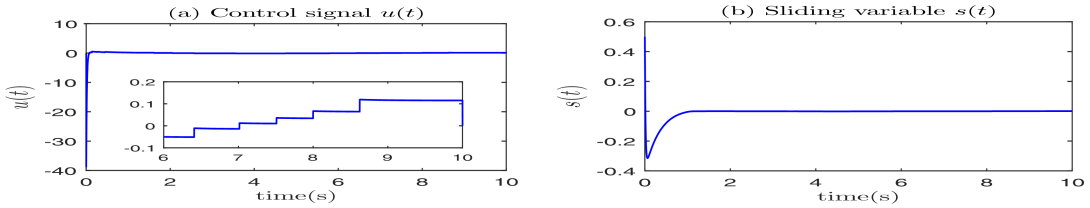

Fig. 3. Control signal $u(t)$ and variables $s(t)$ with $\bar{\mu} = 0.8$.

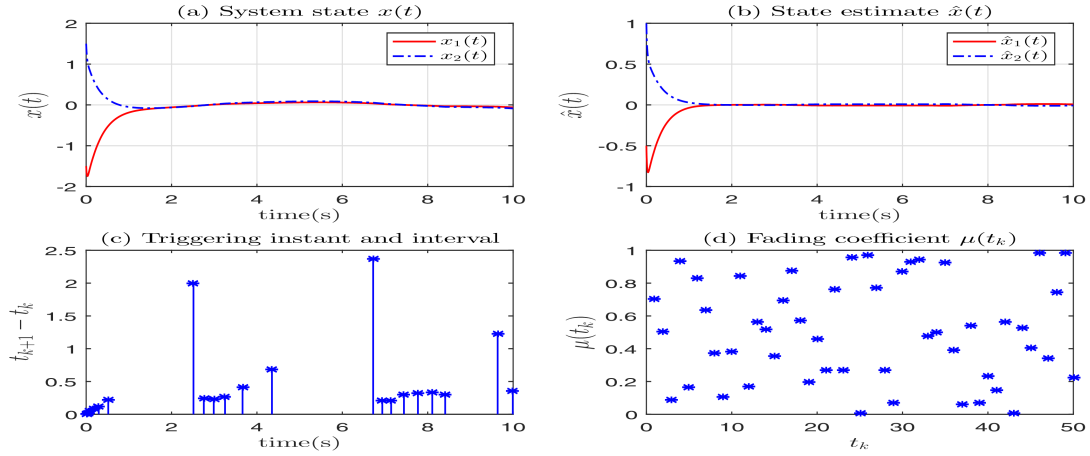

Fig. 4. States $x(t)$ and estimates $\hat{x}(t)$ with $\bar{\mu} = 0.5$.

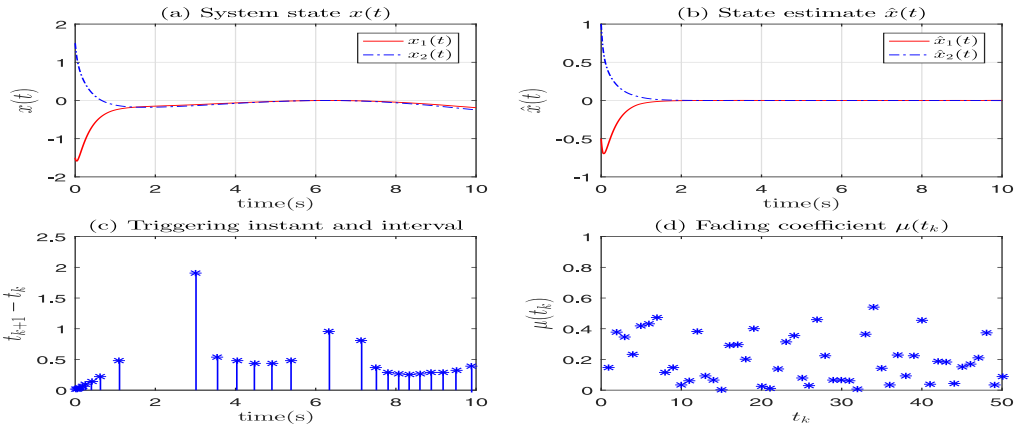

Fig. 5. States $x(t)$ and estimates $\hat{x}(t)$ with $\bar{\mu} = 0.2$.

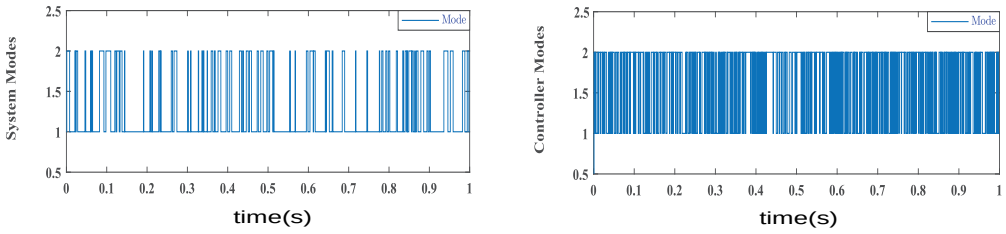

Fig. 6. The evolution of system mode and controller mode

Table 1 displays the triggering numbers, and it can be shown that the smaller $\bar{\lambda}$, in other words, the inferior channel will result in the more event triggering and the slower convergence . In reality, a smaller $\bar{\lambda}$ indicates that the network transmission performance is more prone to channel fading and that the controller is unable to acquire exact signals. Therefore, with the deterioration of the network from $\bar{\lambda}$ =0.8 to $\bar{\lambda}$ =0.2, additional more event triggering will be required for compensating for the performance lost. This has also verified on the basis of simulations and the number of event triggering in Table 1.

5 CONCLUSIONS

In the article, we have researched observer-based finite-time PET SMC for interval type-II S-MJSs affected by quantization and fading channels. In order to save network bandwidth, we introduce quantization and an event-triggered protocol. The mismatched membership functions and the asynchronous problem between the system and the controller are solved, and we obtain less conservative stability conditions. Thereafter, a feasible fuzzy observer-based SMC law is developed, which enables the state trajectories of the system to reach the specified sliding surface within finite-time. And with the aid of the time partition strategy, sufficient conditions for the system to be bounded in finite-time during the arrival and sliding stages are derived. In addition, the suitable fuzzy controller and observer have been obtained. At last, an example is given to verify the validity of the presented approach. In the future, we will apply the theory to multiagent systems and combine different communication protocols, such as the weighted try-once-discard protocol.

FUNDING

This work was supported in part by the National Natural Science Foundation of China under Grants 11661028; the Natural Science Foundation of Guangxi, PR China under Grants 2020GXNSFAA159141.

COMPETING INTERESTS

Authors have declared that no competing interests exist.

REFERENCES

[1] Chen M, Lam HK, Xiao B, Xuan C. Membership-function-dependent control design and stability analysis of interval type-2 sampled-data fuzzy-model-based control system. IEEE Transactions on Fuzzy Systems. 2021;30(6):1614-23.
DOI: 10.1109/TFUZZ.2021.3062898.

[2] Kuppusamy S, Joo YH. Memory-based integral sliding-mode control for T–S fuzzy systems with PMSM via disturbance observer. IEEE Transactions on Cybernetics. 2019;51(5):2457-65.
DOI: 10.1109/TCYB.2019.2953567.

[3] Zhang Z, Niu Y, Lam HK. Sliding-mode control of T–S fuzzy systems under weighted try-once-discard protocol. IEEE transactions on Cybernetics. 2019;50(12):4972-82.
DOI: 10.1109/TCYB.2019.2941870.

[4] Cao Z, Niu Y, Lam HK, Zhao J. Sliding mode control of Markovian jump fuzzy systems: A dynamic event-triggered method. IEEE Transactions on Fuzzy Systems. 2020;29(10):2902-15.
DOI: 10.1109/TFUZZ.2020.3009729.

[5] Ran G, Li C, Sakthivel R, Han C, Wang B, Liu J. Adaptive event-triggered asynchronous control for interval type-2 fuzzy Markov jump systems with cyberattacks. IEEE Transactions on Control of Network Systems. 2022;9(1):88-99.
DOI: 10.1109/TCNS.2022.3141025.

[6] Wang Y, Yan H, Zhang H, Shen H, Lam HK. Interval type-2 fuzzy control for HMM-based multiagent systems via dynamic event-triggered scheme. IEEE Transactions on Fuzzy Systems. 2021;30(8):3063-73.
DOI: 10.1109/TFUZZ.2021.3101581.

[7] Wang J, Xia J, Shen H, Xing M, Park JH. $\mathcal{H}_\infty$ Synchronization for Fuzzy Markov Jump Chaotic Systems With Piecewise-Constant Transition Probabilities Subject to PDT Switching Rule. IEEE Transactions on Fuzzy Systems. 2020;29(10):3082-92. DOI: 10.1109/TFUZZ.2020.3012761.

[8] Zhang M, Shi P, Shen C, Wu ZG. Static output feedback control of switched nonlinear systems with actuator faults. IEEE Transactions on Fuzzy Systems. 2019;28(8):1600-9.
DOI: 10.1109/TFUZZ.2019.2917177.

[9] Yang H, Yin S. Actuator and sensor fault estimation for time-delay Markov jump systems with application to wheeled mobile manipulators. IEEE Transactions on Industrial Informatics. 2019;16(5):3222-32.

[10] Xu Y, Wu ZG, Sun J. Security-based passivity analysis of Markov jump systems via asynchronous triggering control. IEEE Transactions on Cybernetics. 2021 Jul 8;53(1):151-60.
DOI: 10.1109/TCYB.2021.3090398.

[11] Zeng P, Deng F, Zhang H, Gao X. Event-Based H_∞ Control for Discrete-Time Fuzzy Markov Jump Systems Subject to DoS Attacks. IEEE Transactions on Fuzzy Systems. 2021 Mar 29;30(6):1853-63. DOI: 10.1109/TFUZZ.2021.3069345

[12] Ning Z, Cai B, Weng R, Zhang L, Su SF. Stability and control of fuzzy semi-Markov jump systems under unknown semi-Markov kernel. IEEE Transactions on Fuzzy Systems. 2021;30(7):2452-65. DOI: 10.1109/TFUZZ.2021.3083959.

[13] Wu X, Shi P, Tang Y, Mao S, Qian F. Stability analysis of semi-Markov jump stochastic nonlinear systems. IEEE Transactions on Automatic Control. 2021;67(4):2084-91.
DOI: 10.1109/TAC.2021.3071650.

[14] Wang J, Ru T, Xia J, Shen H, Sreeram V. Asynchronous event-triggered sliding mode control for semi-Markov jump systems within a finite-time interval. IEEE Transactions on Circuits and Systems I: Regular Papers. 2020;68(1):458-68.
DOI: 10.1109/TCSI.2020.3034650.

[15] Shang H, Zong G, Qi W. Security control for networked discrete-time semi-Markov jump systems with round-robin protocol. IEEE Transactions on Circuits and Systems II: Express Briefs. 2021;69(6):2812-6.
DOI: 10.1109/TCSII.2021.3132678.

[16] Wang J, Zhang Y, Su L, Park JH, Shen H. Model-Based Fuzzy $l_2 - l_\infty$ Filtering for Discrete-Time Semi-Markov Jump Nonlinear Systems Using Semi-Markov Kernel. IEEE Transactions on Fuzzy Systems. 2021;30(7):2289-99.
DOI: 10.1109/TFUZZ.2021.3078832.

[17] Wang Y, Xu S, Ahn CK. Almost sure finite-time control for Markovian jump systems under asynchronous switching with applications: A sliding mode approach. IEEE Transactions on Circuits and Systems I: Regular Papers. 2022;69(9):3726-35.
DOI: 10.1109/TCSI.2022.3179438.

[18] Su X, Wang C, Chang H, Yang Y, Assawinchaichote W. Event-triggered sliding mode control of networked control systems with Markovian jump parameters. Automatica. 2021;125:109405.
Available: https://doi.org/10.1016/j.automatica.2020.109405.

[19] Song X, Wang M, Ahn CK, Song S. Finite-time H_∞ asynchronous control for nonlinear Markov jump distributed parameter systems via quantized fuzzy output-feedback approach, IEEE Trans. Cybern. 2020;50(9):4098-C4109.

[20] Zhao N, Shi P, Xing W, Lim CP. Resilient adaptive event-triggered fuzzy tracking control and filtering for nonlinear networked systems under denial-of-service attacks. IEEE Transactions on Fuzzy Systems. 2021;30(8):3191-201.
DOI: 10.1109/TFUZZ.2021.3106674.

[21] Zhang L, Guo G. Observer-based adaptive event-triggered sliding mode control of saturated nonlinear networked systems with cyber-attacks. Information Sciences. 2021;543:180-201.
Available: https://doi.org/10.1016/j.ins.2020.06.073

[22] Fan X, Wang Z. Asynchronous event-triggered fuzzy sliding mode control for fractional order fuzzy systems. IEEE Transactions on Circuits and Systems II: Express Briefs. 2021;69(3):1094-8.
DOI: 10.1109/TCSII.2021.3099530.

[23] Li A, Ahn CK, Liu M. T–S Fuzzy-Based Event-Triggering Attitude-Tracking Control for Elastic Spacecraft With Quantization. IEEE Transactions on Aerospace and Electronic Systems. 2021;58(1):124-39.
doi: 10.1109/TAES.2021.3097952.

[24] Xie X, Sheng T, He L. Distributed Event-Triggered Attitude Consensus Control for Spacecraft Formation Flying With Unknown Disturbances and Uncertainties. IEEE Transactions on Aerospace and Electronic Systems. 2021;58(3):1721-32.
DOI: 10.1109/TAES.2021.3120687.

[25] Ma B, Wang Y. Adaptive output feedback control of steer-by-wire systems with event-triggered communication. IEEE/ASME Transactions on Mechatronics. 2021;26(4):1968-79.
DOI: 10.1109/TMECH.2021.3082935.

[26] Yuan Z, Xiong Y, Sun G, Liu J, Wu L. Event-triggered quantized communication-based consensus in multiagent systems via sliding mode. IEEE Transactions on Cybernetics. 2020;52(5):3925-35.
DOI: 10.1109/TCYB.2020.3017550.

[27] Yao D, Li H, Lu R, Shi Y. Distributed sliding-mode tracking control of second-order nonlinear multiagent systems: An event-triggered approach. IEEE Transactions on Cybernetics. 2020;50(9):3892-902.
DOI: 10.1109/TCYB.2019.2963087.

[28] Nie R, He W, Du W, Lang Z, He S. Dynamic event-triggered SMC of multi-agent systems for consensus tracking. IEEE Transactions on Circuits and Systems II: Express Briefs. 2021;69(3):1188-92.
DOI: 10.1109/TCSII.2021.3102331.

[29] Li J, Niu Y, Yang Y. Quantized sliding mode control under hidden Markov digital block-fading channels. Journal of the Franklin Institute. 2021;358(11):5862-82.
Available: https://doi.org/10.1016/j.jfranklin.2021.05.031

[30] Wang J, Yang C, Xia J, Wu ZG, Shen H. Observer-based sliding mode control for networked fuzzy singularly perturbed systems under weighted try-once-discard protocol. IEEE Transactions on Fuzzy Systems. 2021 Mar 31;30(6):1889-99.
DOI: 10.1109/TFUZZ.2021.3070125.

[31] Liu W, Quevedo DE, Vucetic B, Li Y. Stability Conditions for Remote State Estimation of Multiple Systems Over Semi-Markov Fading Channels. IEEE Control Systems Letters. 2022;6:2954-9.
DOI: 10.1109/LCSYS.2022.3181721.

[32] Anjos G, Castanheira D, Silva A, Gameiro A. A Method Exploiting the Channel-Training Phase to Achieve Secrecy in a Fading Broadcast Channel. IEEE Transactions on Signal and Information Processing over Networks. 2022;8:244-57.
DOI: 10.1109/TSIPN.2022.3161086.

[33] Zhang Z, Su SF, Niu Y. Dynamic event-triggered control for interval type-2 fuzzy systems under fading channel. IEEE Transactions on Cybernetics. 2020 Jun 11;51(11):5342-51.
DOI: 10.1109/TCYB.2020.2996296.

[34] Yang Y, Niu Y, Zhang Z. Dynamic event-triggered sliding mode control for interval type-2 fuzzy systems with fading channels. ISA transactions. 2021;110:53-62.
Available: https://doi.org/10.1016/j.isatra.2020.10.035

[35] Huang S, Wang J, Xiong L, Liu J, Li P, Wang Z, Yao G. Fixed-time backstepping fractional-order sliding mode excitation control for performance improvement of power system. IEEE Transactions on Circuits and Systems I: Regular Papers. 2021;69(2):956-69.
DOI: 10.1109/TCSI.2021.3117072.

[36] Y Hu Y, Yan H, Zhang H, Wang M, Zeng L. Robust adaptive fixed-time sliding-mode control for uncertain robotic systems with input saturation. IEEE Transactions on Cybernetics; 2022.
DOI: 10.1109/TCYB.2022.3164739.

[37] Dong B, Ding G, Zhang J, Li Y. Decentralized integral sliding mode control for modular and reconfigurable robot with harmonic drive transmission based on joint torque estimation. In The 27th Chinese Control and Decision Conference (2015 CCDC) 2015; 6167-6174. IEEE.
DOI: 10.1109/CCDC.2015.7161920.

[38] Zhang Z, Niu Y, Cao Z, Song J. Security sliding mode control of interval type-2 fuzzy systems subject to cyber attacks: The stochastic communication protocol case. IEEE Transactions on Fuzzy Systems. 2020 Feb 10;29(2):240-51.
DOI: 10.1109/TFUZZ.2020.2972785.

[39] Song J, Niu Y, Lam HK. Reliable sliding mode control of fast sampling singularly perturbed systems: A redundant channel transmission protocol approach. IEEE Transactions on Circuits and Systems I: Regular Papers. 2019;66(11):4490-501.
DOI: 10.1109/TCSI.2019.2929554.

[40] Zhang Z, Niu Y, Karimi HR. Sliding mode control of interval type-2 fuzzy systems under round-robin scheduling protocol. IEEE Transactions on Systems, Man, and Cybernetics: Systems. 2019;51(12):7602-12.
DOI: 10.1109/TSMC.2019.2956714.

[41] Wang X, Ma Y. Observer-based finite-time asynchronous sliding mode control for Markov jump systems with time-varying delay. Journal of the Franklin Institute. 2022 Jul 1;359(11):5488-511.
Available: https://doi.org/10.1016/j.jfranklin.2022.05.010

[42] Zhang Z, Song J, Zou Y, Niu Y. Finite-time Boundedness of TS Fuzzy Systems Subject to Injection Attacks: A Sliding Mode Control Method. IFAC-PapersOnLine. 2020 Jan 1;53(2):5075-80.
Available: https://doi.org/10.1016/j.ifacol.2020.12.1118

[43] Xu J, Niu Y, Zou Y. Finite-time consensus for singularity-perturbed multiagent system via memory output sliding-mode control. IEEE Transactions on Cybernetics. 2021;52(9):8692-702. DOI: 10.1109/TCYB.2021.3051366.

[44] Qi W, Zong G, Karimi HR. Finite-time observer-based sliding mode control for quantized semi-Markov switching systems with application. IEEE Transactions on Industrial Informatics. 2019;16(2):1259-71.
DOI: 10.1109/TII.2019.2946291.

APPENDIX

Appendix A:

Combined with (10), we can get the derivative of $V_2(t)$ in **Theorem 3.2**:

$$\begin{aligned}\Gamma V_2(t) \leq\ & \tilde{x}^T(t)\{\xi_{1m}P_{1m}^2 + \sum_{n=1}^{M_1}\breve{\pi}_{mn}P_{1n} + Q_{1m} + \bar{\rho}Q_1 + \xi_{1m}^{-1}A_{im}^TA_{im}\}\tilde{x}(t) + \tilde{x}^T(t)\{-\xi_{1m}^{-1}A_{im}^TL_{jm}C_m\}\\ & \tilde{x}(t-\rho(t)) + \tilde{x}^T(t-\rho(t))\{-\xi_{1m}^{-1}C_m^TL_{jm}^TA_{im}\}\tilde{x}(t) + \tilde{x}^T(t-\rho(t))\{\xi_{1m}^{-1}C_m^TL_{jm}^TL_{jm}C_m - (1-g)\\ & Q_{1m}\}\tilde{x}(t-\rho(t)) + \tilde{x}^T(t)\{-\bar{\lambda}P_{1m}L_{jm}\}e_k(t) + e_k^T(t)\{-\bar{\lambda}L_{jm}^TP_{1m}\}\tilde{x}(t) + \tilde{x}^T(t)\{-\bar{\lambda}P_{1m}L_{jm}\}\\ & Q(y(t_kh+\varepsilon h)) + Q^T(y(t_kh+\varepsilon h))\{-\bar{\lambda}L_{jm}^TP_{1m}\}\tilde{x}(t) + \tilde{x}^T(t)\{P_{1m}L_{jm}C_m\}x(t-\rho(t))\\ & +x^T(t-\rho(t))\{C_m^TL_{jm}^TP_{1m}\}\tilde{x}(t) + \hat{x}^T(t)\{P_{2m}A_{im} + A_{im}^TP_{2m} + P_{2m}\sum_{l=1}^{M_2}\hat{\pi}_{ml}B_{im}K_{ml}\\ & + \sum_{l=1}^{M_2}\hat{\pi}_{ml}K_{ml}^TB_{im}^T + \sum_{n=1}^{M_1}\breve{\pi}_{mn}P_{2n} + Q_{2m} + \bar{\rho}Q_2\}\hat{x}(t) + \tilde{x}^T(t)P_{1m}\bar{w}(t) + \bar{w}^T(t)P_{1m}\tilde{x}(t)\\ & +\hat{x}^T(t)\{-P_{2m}\tilde{B}_{im}L_{jm}C_m\}\hat{x}(t-\rho(t)) + \hat{x}^T(t-\rho(t))\{-C_m^TL_{jm}^T\tilde{B}_{im}^TP_{2m}\}\hat{x}(t)\\ & -(1-g)\hat{x}^T(t-\rho(t))Q_{2m}\hat{x}(t-\rho(t)) + \hat{x}^T(t)\{P_{2m}\tilde{B}_{im}L_{jm}\}\bar{y}(t) + \bar{y}^T(t)\{L_{jm}^T\tilde{B}_{im}^TP_{2m}\}\hat{x}(t)\\ & -\hat{x}^T(t)\{P_{2m}B_{im}\}\bar{\partial}(t) - \bar{\partial}^T(t)\{B_{im}^TP_{2m}\}\hat{x}(t) - e_k^T(t)\Phi_me_k(t) + \alpha_mQ^T(y(t-\rho(t)))\Phi_mQ(y(t-\rho(t)))\end{aligned}$$

Then by Schur complement [5] and $(32) \sim (34)$, we can get

$$\sum_{i=1}^{v}\sum_{j=1}^{v}\eta_i\theta_j\Theta_{ij} = \begin{bmatrix}\diamondsuit_1 & \diamondsuit_2 & \diamondsuit_3 & \diamondsuit_4 & \diamondsuit_5 & \diamondsuit_6 & \diamondsuit_7 & \diamondsuit_8 & \diamondsuit_9 & \diamondsuit_{10} & \diamondsuit_{11}\end{bmatrix} \tag{67}$$

where

$$\begin{aligned}\diamondsuit_1 &= \begin{bmatrix}Z_{11m}^{(1)\ T} & (-\xi_{1m}^{-1}A_{im}^TL_{jm}C_m)^T & 0 & 0 & V_{15m}^{(1)\ T} & 0 & 0 & V_{18m}^{(1)\ T} & V_{19m}^{(1)\ T} & P_{1m} & 0\end{bmatrix}^T\\ \diamondsuit_2 &= \begin{bmatrix}(-\xi_{1m}^{-1}A_{im}^TL_{jm}C_m)^T & -(1-g)Q_{1m} + (\xi_{1m}^{-1}C_m^TL_{jm}^TL_{jm}C_m)^T & 0 & 0 & 0 & 0 & 0 & 0 & 0 & 0\end{bmatrix}^T\\ \diamondsuit_3 &= \begin{bmatrix}0 & 0 & V_{33m}^{(1)\ T} & V_{34m}^{(1)\ T} & 0 & 0 & V_{37m}^{(1)\ T} & 0 & 0 & 0 & -(P_{2m}B_{im})^T\end{bmatrix}^T\\ \diamondsuit_4 &= \begin{bmatrix}0 & 0 & V_{34m}^{(1)\ T} & -(1-g)Q_{2m} & 0 & 0 & 0 & 0 & 0 & 0 & 0\end{bmatrix}^T\\ \diamondsuit_5 &= \begin{bmatrix}V_{15m}^{(1)\ T} & 0 & 0 & 0 & -\Phi_m & 0 & 0 & 0 & 0 & 0 & 0\end{bmatrix}^T\\ \diamondsuit_6 &= \begin{bmatrix}0 & 0 & 0 & 0 & 0 & \alpha_m\Phi_m - \xi_mI & 0 & 0 & 0 & 0 & 0\end{bmatrix}^T\\ \diamondsuit_7 &= \begin{bmatrix}0 & 0 & V_{37m}^{(1)\ T} & 0 & 0 & 0 & -\xi_mI & 0 & 0 & 0 & 0\end{bmatrix}^T\\ \diamondsuit_8 &= \begin{bmatrix}V_{18m}^{(1)\ T} & 0 & 0 & 0 & 0 & 0 & 0 & -\xi_mI & 0 & 0 & 0\end{bmatrix}^T\\ \diamondsuit_9 &= \begin{bmatrix}V_{19m}^{(1)\ T} & 0 & 0 & 0 & 0 & 0 & 0 & 0 & -\xi_mI & 0 & 0\end{bmatrix}^T\\ \diamondsuit_{10} &= \begin{bmatrix}P_{1m} & 0 & 0 & 0 & 0 & 0 & 0 & 0 & 0 & -\xi_mI & 0\end{bmatrix}^T\\ \diamondsuit_{11} &= \begin{bmatrix}0 & 0 & (-P_{2m}B_{im})^T & 0 & 0 & 0 & 0 & 0 & 0 & 0 & -\xi_mI\end{bmatrix}^T\end{aligned}$$

$Z_{11m}^{(1)} = V_{11m}^{(1)} + \xi_{1m}^{-1}A_{im}{}^TA_{im} + \xi_{1m}P_m^2$

Let

$$\begin{aligned}\spadesuit(t) = \begin{bmatrix}\tilde{x}(t) & \tilde{x}(t-\rho(t)) & \hat{x}(t) & \hat{x}(t-\rho(t)) & e_k(t) & Q(y(t-\rho(t)))\\ \bar{y}(t) & x(t-\rho(t)) & Q(y(t_kh+\varepsilon h)) & \bar{w}(t) & \bar{\partial}(t) & \end{bmatrix}^T\end{aligned}$$

Therefore, the following inequality holds:

$$\begin{aligned}&H_1(t) = \Gamma V_2(t) - \xi_mV_2(t) - \xi_m\bar{w}^T(t)\bar{w}(t) - \xi_m\bar{\partial}^T(t)\bar{\partial}(t) - \xi_m\bar{y}^T(t)\bar{y}(t) - \xi_mx^T(t-\rho(t))x(t-\rho(t))\\ &-\xi_mQ^T(y(t-\rho(t)))Q(y(t-\rho(t))) - \xi_mQ^T(y(t_kh+\varepsilon h))Q(y(t_kh+\varepsilon h)) \leq \spadesuit^T(t)\Theta_{ij}\spadesuit(t) < 0\end{aligned} \tag{68}$$

Then, we have

$$\begin{aligned}\Gamma V_2(t) \leq \xi_m V_2(t) + \xi_m \bar{w}^T(t)\bar{w}(t) + \xi_m \bar{\partial}^T(t)\bar{\partial}(t) + \xi_m \bar{y}^T(t)\bar{y}(t) + \xi_m x^T(t-\rho(t))x(t-\rho(t)) \\ +\xi_m Q^T(y(t-\rho(t)))Q(y(t-\rho(t))) + \xi_m Q^T(y(t_k h+\varepsilon h))Q(y(t_k h+\varepsilon h))\end{aligned} \tag{69}$$

So as to make full use of MFs information and reduce the conservativeness, slack matrices Λ_i are introduced. By using the property of MFs, i.e., $\sum\limits_{i=1}^{v}\eta_i(x(t)) = 1$,we obtain:

$$\sum_{i=1}^{v}\sum_{j=1}^{v}\eta_i(\eta_j-\theta_j)\Lambda_i = \sum_{i=1}^{v}\eta_i(\sum_{j=1}^{v}\eta_j - \sum_{j=1}^{v}\theta_j)\Lambda_i = 0 \tag{70}$$

In accordance with (67) and (70) and Schur complement,we get that:

$$\begin{aligned}&\sum_{i=1}^{v}\sum_{j=1}^{v}\eta_i\theta_j\Theta_{ij}^* \\ &= \sum_{i=1}^{v}\sum_{j=1}^{v}\eta_i\theta_j\Theta_{ij}^* + \sum_{i=1}^{v}\sum_{j=1}^{v}\eta_i(\eta_j-\theta_j)\Lambda_i \\ &= \sum_{i=1}^{v}\sum_{j=1}^{v}\eta_i\theta_j(\Theta_{ij}^*-\Lambda_i) + \sum_{i=1}^{v}\sum_{j=1}^{v}\eta_i\eta_j\Lambda_i \\ &= \sum_{i=1}^{v}\sum_{j=1}^{v}\eta_i(\theta_j-k_j\Lambda_j)(\Theta_{ij}^*-\Lambda_i) + \sum_{i=1}^{v}\sum_{j=1}^{v}\eta_i\eta_j(k_j(\Theta_{ij}^*-\Lambda_i)+\Lambda_i) \\ &= \sum_{i=1}^{v}\sum_{j=1}^{v}\eta_i(\theta_j-k_j\eta_j)(\Theta_{ij}^*-\Lambda_i) + \sum_{i=1}^{v}\sum_{j=1}^{v}\eta_i\eta_j(k_j\Theta_{ij}^*+(1-k_j)\Lambda_i) \\ &= \sum_{i=1}^{v}\sum_{j=1}^{v}\eta_i(\theta_j-k_j\eta_j)(\Theta_{ij}^*-\Lambda_i) + \sum_{i=1}^{v}\eta_i^2(k_i\Theta_{ii}^*+(1-k_i)\Lambda_i) \\ &\qquad + \sum_{i=1}^{v}\sum_{j>i}^{v}\eta_i\eta_j[k_j\Theta_{ij}^*+(1-k_j)\Lambda_i + k_i\Theta_{ji}^*+(1-k_i)\Lambda_j]\end{aligned} \tag{71}$$

By virtue of $(32)\sim(34)$,we can get that $(71)<0$.

Appendix B:

Combined with (10), we can get the derivative of $V_2(t)$ in **Theorem 3.3**:

$$\begin{aligned}\Gamma V_3(t) \leq\ & \tilde{x}^T(t)\{\xi_{1m}P_{1m}^2 + \sum_{n=1}^{M_1}\breve{\pi}_{mn}P_{1n} + Q_{1m} + \bar{\rho}Q_1 + \xi_{1m}^{-1}A_{im}^TA_{im}\}\tilde{x}(t) + \tilde{x}^T(t)\{-\xi_{1m}^{-1}A_{im}^TL_{jm}C_m\} \\ & \tilde{x}(t-\rho(t)) + \tilde{x}^T(t-\rho(t))\{-\xi_{1m}^{-1}C_m^TL_{jm}^TA_{im}\}\tilde{x}(t) + \tilde{x}^T(t-\rho(t))\{\xi_{1m}^{-1}C_m^TL_{jm}^TL_{jm}C_m - (1-g) \\ & Q_{1m}\}\tilde{x}(t-\rho(t)) + \tilde{x}^T(t)\{-\bar{\lambda}P_{1m}L_{jm}\}e_k(t) + e_k^T(t)\{-\bar{\lambda}L_{jm}^TP_{1m}\}\tilde{x}(t) + \tilde{x}^T(t)\{-\bar{\lambda}P_{1m}L_{jm}\} \\ & Q(y(t_kh+\varepsilon h)) + Q^T(y(t_kh+\varepsilon h))\{-\bar{\lambda}L_{jm}^TP_{1m}\}\tilde{x}(t) + \tilde{x}^T(t)\{P_{1m}L_{jm}C_m\}x(t-\rho(t)) \\ & +x^T(t-\rho(t))\{C_m^TL_{jm}^TP_{1m}\}\tilde{x}(t) + \hat{x}^T(t)\{P_{2m}A_{im} + A_{im}^TP_{2m} + P_{2m}\sum_{l=1}^{M_2}\hat{\pi}_{ml}B_{im}K_{ml} \\ & +\sum_{l=1}^{M_2}\hat{\pi}_{ml}K_{ml}^TB_{im}^T + \sum_{n=1}^{M_1}\breve{\pi}_{mn}P_{2n} + Q_{2m} + \bar{\rho}Q_2\}\hat{x}(t) + \tilde{x}^T(t)P_{1m}\bar{w}(t) + \bar{w}^T(t)P_{1m}\tilde{x}(t) \\ & +\hat{x}^T(t)\{-P_{2m}\tilde{B}_{im}L_{jm}C_m\}\hat{x}(t-\rho(t)) + \hat{x}^T(t-\rho(t))\{-C_m^TL_{jm}^T\tilde{B}_{im}^TP_{2m}\}\hat{x}(t) \\ & -(1-g)\hat{x}^T(t-\rho(t))Q_{2m}\hat{x}(t-\rho(t)) + \hat{x}^T(t)\{P_{2m}\tilde{B}_{im}L_{jm}\}\bar{y}(t) + \bar{y}^T(t)\{L_{jm}^T\tilde{B}_{im}^TP_{2m}\}\hat{x}(t) \\ & -e_k^T(t)\Phi_me_k(t) + \alpha_mQ^T(y(t-\rho(t)))\Phi_mQ(y(t-\rho(t)))\end{aligned}$$

By Schur comlement [5] and $(48)\sim(50)$, the subsequent steps are analogous to those in **Appendix A**.

Next,

$$H_2(t) = \Gamma V_3(t) - \xi_m V_3(t) - \xi_m \bar{w}^T(t)\bar{w}(t) - \xi_m \bar{y}^T(t)\bar{y}(t) - \xi_m x^T(t-\rho(t))x(t-\rho(t)) \\ -\xi_m Q^T(y(t-\rho(t)))Q(y(t-\rho(t))) - \xi_m Q^T(y(t_k h+\varepsilon h)Q(y(t_k h+\varepsilon h)) \tag{72}$$

Thus,

$$\Gamma V_3(t) \leq \xi_m V_3(t) + \xi_m \bar{w}^T(t)\bar{w}(t) + \xi_m \bar{y}^T(t)\bar{y}(t) + \xi_m x^T(t-\rho(t))x(t-\rho(t)) \\ +\xi_m Q^T(y(t-\rho(t)))Q(y(t-\rho(t))) + \xi_m Q^T(y(t_k h+\varepsilon h))Q(y(t_k h+\varepsilon h)) \tag{73}$$

Peer-review history:
The peer review history for this paper can be accessed here:
https://www.sdiarticle5.com/review-history/97150